3-Phenyl-Substituted Imidazo[1,5-*a*]quinoxalin-4-ones and Imidazo[1,5-*a*]quinoxaline Ureas That Have High Affinity at the $GABA_A$/Benzodiazepine Receptor Complex†

E. Jon Jacobsen,*,‡ Lindsay S. Stelzer,‡ Kenneth L. Belonga,‡ Donald B. Carter,§ Wha Bin Im,§ Vimala H. Sethy,§ Andrew H. Tang,§ Philip F. VonVoigtlander,§ and James D. Petke⊥

Departments of Structural and Medicinal Chemistry, Central Nervous System Diseases Research, and Computational Chemistry, Pharmacia & Upjohn, Kalamazoo, Michigan 49001

Received January 22, 1996⊗

A series of imidazo[1,5-*a*]quinoxalin-4-ones and imidazo[1,5-*a*]quinoxaline ureas containing substituted phenyl groups at the 3-position was developed. Compounds within the imidazo-[1,5-*a*]quinoxaline urea series had high affinity for the $GABA_A$/benzodiazepine receptor complex with varying *in vitro* efficacy, although most analogs were partial agonists as indicated by [^{35}S]TBPS and Cl^- current ratios. Interestingly, a subseries of piperazine ureas was identified which had biphasic efficacy, becoming more antagonistic with increasing concentration. Analogs within the imidazo[1,5-*a*]quinoxalin-4-one series had substantially decreased binding affinity as compared to the quinoxaline urea series. These compounds ranged from antagonists to full agonists by *in vitro* analysis, with several derivatives having roughly 4-fold greater intrinsic activity than diazepam as indicated by Cl^- current measurement. Numerous compounds from both series were effective in antagonizing metrazole-induced seizures, consistent with anticonvulsant properties and possible anxiolytic activity. Most of the quinoxaline ureas and quinoxalin-4-ones were active in an acute electroshock physical dependence side effect assay in mice precluding further development.

Introduction

The excitability of many central nervous system (CNS) pathways is controlled by the action of γ-aminobutyric acid (GABA) on the $GABA_A$ chloride ion channel complex.[1] Of the chemical classes which have binding sites on this macromolecular ionophore, the benzodiazepines are the most widely studied. Ligands which interact with the benzodiazepine receptor (BzR) and allosterically modulate the action of GABA on neuronal chloride ion flux have a continuum of intrinsic activity,[2] ranging from full agonists (anxiolytic, hypnotic, and anticonvulsant agents) through antagonists to inverse agonists (proconvulsant and anxiogenic agents). Partial agonists exist within this continuum and may be devoid of typical benzodiazepine-mediated side effects such as physical dependence, ethanol potentiation, amnesia, oversedation (for anxiolytic agents), and muscle relaxation or, in the case of inverse agonists, convulsive activity.[3] Furthermore, several different receptor subunits (α, β, γ, δ) combine to form the $GABA_A$ receptor complex,[4] with at least three to four native receptor subtypes identified thus far.[5] The possibility that subtype selective ligands may discriminate between useful anxiolytic or hypnotic activity and overt side effects may also allow for improved medications.

We recently reported on a series of high-affinity partial agonist imidazo[1,5-*a*]quinoxalines which were appended with amide, urea, carbamate, and thiocarbamate side chains.[6] Selected compounds such as **1** (U-91571; Figure 1) displayed excellent antianxiety activity in animal models yet had limited benzodiazepine-type side effects.[6b] This series, in part, arose from a structure−activity relationship (SAR) evaluation of a class of imidazo[1,5-*a*]quinoxalin-4-ones, of which **2** (U-78875) was the lead compound.[7] Unfortunately **2** was removed from clinical trials for the treatment of anxiety due to increases in liver enzymes. Detailed toxicological evaluation of **2** subsequently indicated that the increase in serum triglycerides observed is due to cyclopropanecarboxylic acid, which results from species-dependent metabolism of the oxadiazole group.[8] Compounds containing other groups substituted at the 5′-oxadiazole position, such as *tert*-butyl **4** (U-94000) or the "reverse" O−N oxadiazole **3** (U-95963) as shown in Figure 1, also promoted enzyme induction, whereas methyl, ethyl, and isopropyl substituents did not.[9] Disappointingly, these derivatives containing simple C1−C3 alkyl groups were rapidly metabolized in contrast to **2**. Although **1** had a

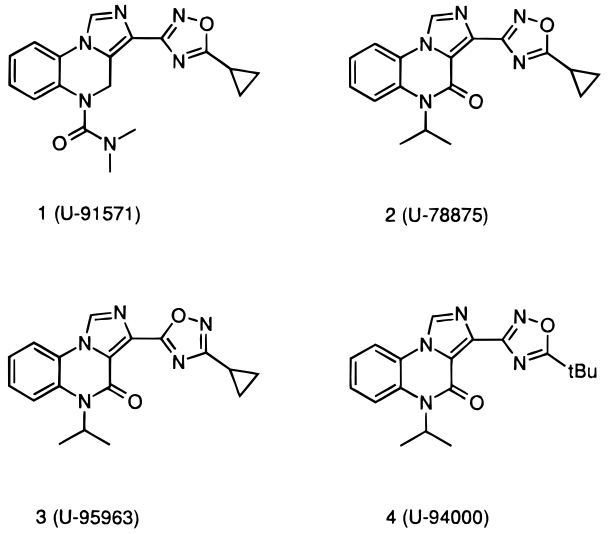

Figure 1. Quinoxalines **1**−**4**.

† A portion of this material was presented at the 207th American Chemical Society National Meeting, March 13−17, 1994.
‡ Department of Structural and Medicinal Chemistry.
§ Department of Central Nervous System Diseases Research.
⊥ Department of Computational Chemistry.
⊗ Abstract published in *Advance ACS Abstracts,* August 15, 1996.

S0022-2623(96)00070-2 CCC: $12.00

Scheme 1[a]

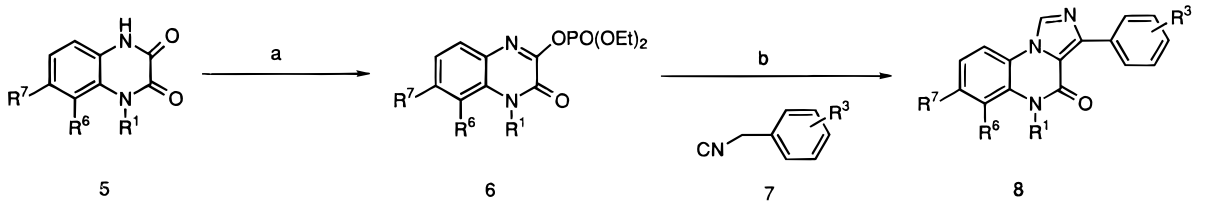

[a] Reagents: (a) tBuOK, THF, diethyl chlorophosphate; (b) tBuOK, **7**.

Scheme 2[a]

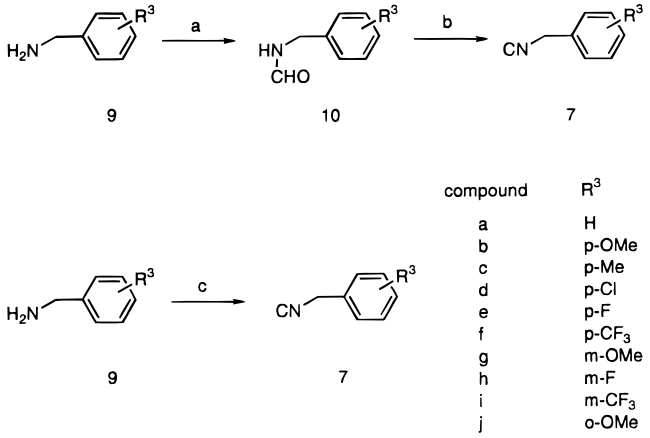

compound	R^3
a	H
b	p-OMe
c	p-Me
d	p-Cl
e	p-F
f	p-CF_3
g	m-OMe
h	m-F
i	m-CF_3
j	o-OMe

[a] Reagents: (a) EtOCHO; (b) $POCl_3$, Et_3N, CH_2Cl_2; (c) 50% NaOH, $CHCl_3$, $BnEt_3NCl$, CH_2Cl_2.

Scheme 3[a]

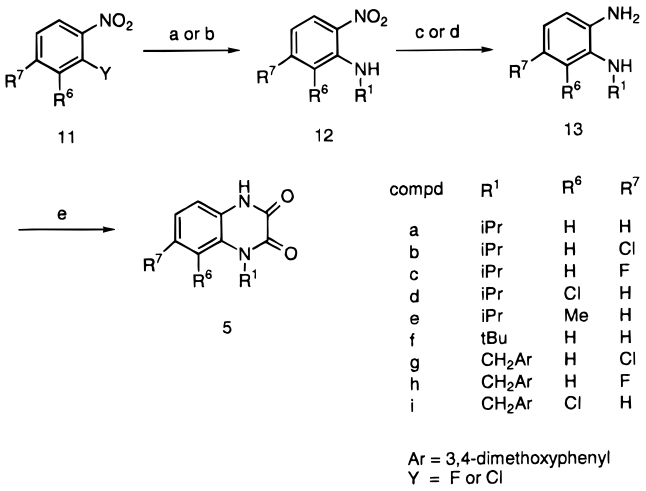

compd	R^1	R^6	R^7
a	iPr	H	H
b	iPr	H	Cl
c	iPr	H	F
d	iPr	Cl	H
e	iPr	Me	H
f	tBu	H	H
g	CH_2Ar	H	Cl
h	CH_2Ar	H	F
i	CH_2Ar	Cl	H

Ar = 3,4-dimethoxyphenyl
Y = F or Cl

[a] Reagents: (a) $iPrNH_2$ or $tBuNH_2$, 150 °C; (b) veratrylamine, $EtNiPr_2$, 75 °C; (c) H_2, 5% Pd/C, EtOH; (d) H_2, Pt/S/C, EtOH; (e) EtOCOCOCl, $EtNiPr_2$, toluene.

significantly different metabolic profile than **2**, concerns over possible degradation of the oxadiazole group to release cyclopropanecarboxylic acid discouraged further interest in this compound.

Within the imidazole benzodiazepine template, numerous functional groups have been appended at the 3-position to control affinity and modulate efficacy.[10,11] Most notable are esters (from which the oxadiazoles were derived), amides, oxadiazoles, thiazoles, furans, thiophenes, and phenyl rings. Typically compounds with ester, oxadiazole, or furan substituents have greater affinity to the benzodiazepine/$GABA_A$ receptor complex than the other 3-aryl analogs.[10] With the need to reevaluate other non-oxadiazole substituents at the 3-position in the series derived from both **1** and **2**, analogs containing esters, isoxazoles, and substituted phenyl groups were synthesized. In this manuscript we disclose our work directed toward 3-phenylimidazo[1,5-*a*]quinoxalin-4-ones and 3-phenylimidazo[1,5-*a*]quinoxaline ureas, as well as the dramatic effects that this substitution pattern has on affinity and *in vitro* efficacy.

Chemistry

The desired imidazo[1,5-*a*]quinoxalin-4-ones **8** were synthesized as shown in Scheme 1. Reaction of **5** with potassium *tert*-butoxide and diethyl chlorophosphate provided enol phosphate ester **6**. This intermediate **6**, which was usually not isolated, was reacted with the desired isocyanide **7** in the presence of additional potassium *tert*-butoxide to provide **8**.

The aryl isocyanides were prepared by one of two routes as shown in Scheme 2, starting with the desired substituted benzylamine. Reaction of **9** with ethyl formate provided formamide **10** which was dehydrated with phosphorous oxychloride in the presence of triethylamine to provide the isocyanide **7**. Alternatively following the general procedure of Weber,[12] substituted benzylamine **9** was converted to isocyanide **7** directly.

The various 2,3-dioxoquinoxaline templates **5** were prepared as illustrated in Scheme 3 following procedures similar to that developed by Watjen.[13] Reaction of the appropriate 2-halonitrobenzene **11** with isopropylamine provided **12** in excellent yield. Reduction of the nitro group in **12** was accomplished either via catalytic hydrogenation or through the use of Raney nickel or titanium(III) trichloride to provide relatively unstable diamine **13**. Reaction of **13** with ethyl oxalyl chloride at −78 °C in toluene followed by heating the reaction mixture at reflux gave the desired diones **5a**−**e**. Substitution of isopropylamine for either *tert*-butylamine or veratrylamine provided the appropriately substituted 2,3-dioxoquinoxaline templates **5f**−**i**, utilized as starting material in Scheme 5. Table 1 highlights the physical data of the imidazo[1,5-*a*]quinoxalin-4-ones prepared by these methods.

The 3-aryl-substituted imidazo[1,5-*a*]quinoxaline ureas were prepared by two different routes. As shown in Scheme 4, exposure of quinoxaline template[6] **14** to phosgene (or triphosgene) provided a carbamoyl chloride which was reacted directly with an amine to provide urea **15**. Cyclization of **15** using diethyl chlorophosphate, potassium *tert*-butoxide, and isocyanide **7** as detailed above provided imidazo[1,5-*a*]quinoxaline **16**. This sequence was satisfactory when R^4 was methyl, providing **16** in yields of 23−74% (**15** → **16**). However, when R^4 was hydrogen, only a trace amount of **16** was isolated. Presumably in this case, the intermediate enol phosphonate of **17** (R^4 = H) can be deprotonated by the relatively basic isocyanide anion leading to decomposition. In contrast with the *gem*-dimethyl analogs **17** (R^4

Table 1. Physical Data for Imidazo[1,5-*a*]quinoxalin-4-ones

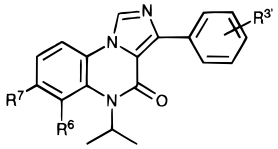

compd	$R^{3'}$	R^6	R^7	mp (°C)	method	yield (%)	formula	anal.
23	H	H	H	207−208	A	52	$C_{19}H_{17}N_3O$	C, H, N
24	4′-OCH_3	H	H	187−189	B	41	$C_{20}H_{19}N_3O_2 \cdot (H_2O)_{1/2}$	C, H, N
25	4′-CH_3	H	H	209−210	A	20	$C_{20}H_{19}N_3O$	C, H, N
26	4′-Cl	H	H	211−212	A	42	$C_{19}H_{16}N_3OCl$	C, H, N, Cl
27	4′-F	H	H	201−202	B	31	$C_{19}H_{16}N_3OF$	C, H, N
28	4′-CF_3	H	H	184−185	B	62	$C_{20}H_{16}N_3OF_3$	C, H, N
29	3′-OCH_3	H	H	180−181	B	78	$C_{20}H_{19}N_3O_2$	C, H, N
30	3′-F	H	H	215−217	B	74	$C_{19}H_{16}N_3OF \cdot (H_2O)_{1/8}$	C, H, N
31	3′-CF_3	H	H	210−211	B	83	$C_{20}H_{16}N_3OF_3$	C, H, N
32	2′-OCH_3	H	H	151−152	B	37	$C_{20}H_{19}N_3O_2$	C, H, N
33	H	H	F	223−224	B	15	$C_{19}H_{16}N_3OF$	C, H, N
34	4′-OCH_3	H	F	>300	B	30	$C_{20}H_{18}N_3O_2F$	C, H, N
35	4′-F	H	F	229−230	B	51	$C_{19}H_{15}N_3OF_2 \cdot (H_2O)_{3/8}$	C, H, N
36	4′-F	H	Cl	286−288	B	43	$C_{19}H_{15}N_3OClF \cdot H_2O$	C, H, N, Cl
37	4′-OCH_3	Cl	H	164−165	B	44	$C_{20}H_{18}N_3O_2Cl$	C, H, N, Cl
38	4′-F	Cl	H	157−158	B	43	$C_{19}H_{15}N_3OClF$	C, H, N, Cl
39	4′-OCH_3	CH_3	H	179−180	B	50	$C_{21}H_{21}N_3O_2$	C, H, N
40	4′-F	CH_3	H	165−166	B	65	$C_{20}H_{18}N_3OF$	C, H, N

Scheme 4[a]

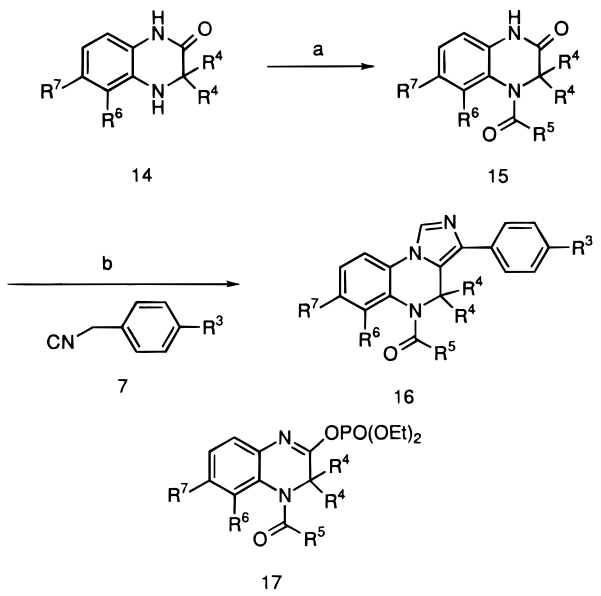

[a] Reagents: (a) phosgene in toluene, CH_2Cl_2, $EtNiPr_2$, R^5H, $EtNiPr_2$; (b) tBuOK, THF, diethyl chlorophosphate, tBuOK, **7**.

= Me), the enol phosphonate does not have an acidic hydrogen and reacts cleanly with the isocyanide anion. Additionally the use of the less basic oxadiazole isocyanide anion, which was used successfully (47−70%) in our previous work,[6] prevents this side reaction.

The use of a blocking group at the 4-position (imidazo[1,5-*a*]quinoxaline numbering) allowed for a successful resolution to this problem as shown in Scheme 5. Protected quinoxaline-2,3-diones **5f**−**i** (R^1 = *tert*-butyl or 3,4-dimethoxybenzyl) were prepared as shown in Scheme 3. The use of veratrylamine as a protecting group at this position was necessary for the halogenated analogs as derivatives of diamine **13f** (R^6 or R^7 = halo) would not cyclize with ethyl oxalyl chloride to provide **5f**−**i** (R^6 or R^7 = halo). The standard imidazole ring-forming reaction was carried out with **5** to provide imidazo[1,5-*a*]quinoxalinones **8a**−**g**. Reduction with borane−methyl sulfide complex or lithium aluminum hydride (LAH) provided amines **18a,b,e**−**g** which were deprotected with trifluoroacetic acid to give the desired template **19**. Occasionally a small amount of the imine of **19** was formed during this step which was reduced with sodium borohydride. An alternative route to **19** was also developed. Deprotection of **8c,d** (R^1 = *tert*-butyl) provided amides **20c**,**d** which were reduced with either LAH or aluminum hydride to give the imidazo[1,5-*a*]quinoxaline **19**. Acylation of **19** with a substituted benzoyl chloride provided amide **21**. Ureas and carbamates were formed by exposure of **19** to phosgene or triphosgene to provide carbamoyl chloride **22**, which, typically without isolation, was reacted with the desired nucleophile (amines, alcohols) to provide **16**. The carbamoyl chloride could also be isolated and stored indefinitely before further reaction. The 3,4,5-trimethylpiperazine analogs **49**, **68**, **70**, and **72** were prepared from their *cis*-3,5-dimethylpiperazine precursors by the reductive amination procedure of Borch.[14] Table 2 highlights the physical data and methods used for the synthesis of the imidazo[1,5-*a*]quinoxaline ureas, amides, and carbamates.

Results and Discussion

The binding affinity of the imidazo[1,5-*a*]quinoxalines at the benzodiazepine receptor in rat cortical membranes was determined by competition experiments with radiolabeled [^{3}H]flunitrazepam (Fnz).[15] The *in vitro* efficacy of these compounds was accessed by two different methods. The TBPS ratio[16] was determined for each compound by measuring its effect on *tert*-butyl bicyclophosphorothionate (TBPS) binding to the picrotoxin convulsant site on the $GABA_A$ chloride complex. Differences in TBPS binding presumably occur due to conformational changes in the chloride ionophore, allosterically modulated by the binding of the test compound to the benzodiazepine receptor. The resultant value, expressed as a ratio of that for the test drug to that of diazepam, is 1 for a full agonist and 0 for an antagonist, with negative values for inverse agonists. A second and more direct measure of *in vitro* efficacy was determined by a Cl^- current assay.[16−18] The

Scheme 5[a]

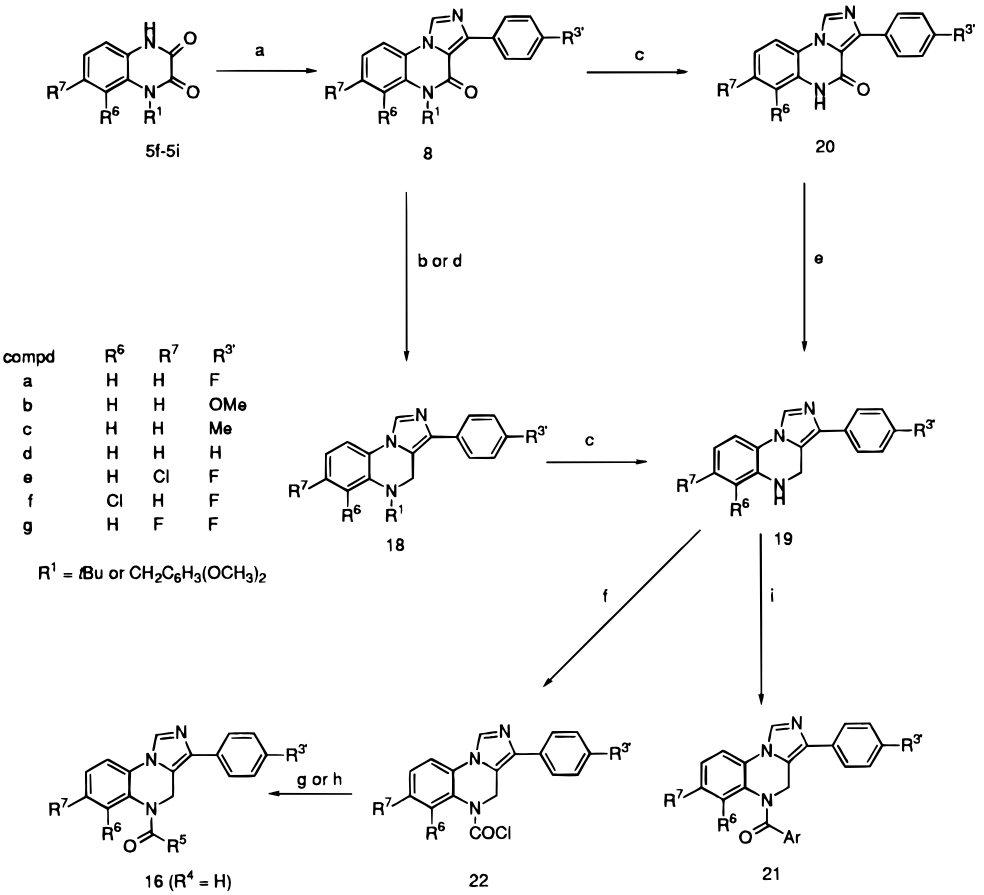

[a] Reagents: (a) tBuOK, THF, diethyl chlorophosphate, tBuOK, **7**; (b) BH_3DMS, THF; (c) TFA, CH_2Cl_2; (d) LAH, THF; (e) AlH_3, THF; (f) phosgene in toluene, $EtNiPr_2$, CH_2Cl_2; (g) R^5H, $EtNiPr_2$, THF; (h) R^5Na, R^5H; (i) ArCOCl, $EtNiPr_2$, THF.

synaptic chloride conductance effected by GABA activating the $GABA_A$ receptor complex is modulated by ligands acting at the benzodiazepine receptor. Full agonists increase GABA-mediated current, and antagonists have no effect while inverse agonists decrease ion flow. The test compounds were again compared to diazepam and thus, like the TBPS assay, had a similar numerical scale. All compounds were evaluated in the $\alpha_1\beta_2\gamma_2$ subtype in this assay. To provide a quick measure of *in vivo* efficacy, most analogs were evaluated for their ability to antagonize metrazole-induced seizures (clonic and tonic).[19] While a direct measure of anticonvulsant activity, this assay is also predictive of possible anxiolytic properties as standard full agonist benzodiazepine (BZD) agents such as diazepam, alprazolam, and zolpidem are extremely effective, as are partial agonists such as **2**, bretazenil, and abercarnil,[20] although to a lesser degree.

For the simple quinoxalin-4-one template (R^6, R^7 = H), replacement of the oxadiazole of **2** with a phenyl ring resulted, for the most part, in dramatically decreased binding affinity (Table 3). The most direct comparison (**23** vs **2**) indicates a 24-fold decrease in receptor affinity. Relatively small groups such as *p*-fluoro and *p*-methyl resulted in an additional 4-fold decrease in affinity, while the larger and more electronegative chloro (**26**) and trifluoromethyl (**28**) derivatives were relatively inactive. However, substitution on the 3-phenyl ring with an electron rich *p*-OMe group did provide slightly enhanced affinity with **24** having a K_i of 32 nM. Substitution at the *meta*-position provided analogs **29**−**31** with low affinity (188−480 nM), while the lone *ortho*-substituted derivative **32** (*o*-OMe) was completely inactive. The substituent on the 3-phenyl ring also had significant effects on *in vitro* efficacy. In the TBPS assay, **23**, **29**, and **30** were nearly antagonists and the 4′-fluoro and 4′-methoxy analogs partial agonists, while *p*-methyl **25** was a full agonist. These compounds were all significantly more agonistic than **2** in this assay. In the chloride current screen, **23** and **26** were antagonists like **2**, while **24**, **25**, and **27** were partial agonists. In the *meta*-series, all three analogs were weak partial agonists or antagonists as indicated by both assays except for **29**, which had similar efficacy to that of diazepam in the chloride current assay. In the metrazole assay, only **24** had reasonable activity (ED_{50} = 12.5 mg/kg), which is consistent with its affinity and chloride current ratio. The *p*-fluoro analog **27** was also (weakly) active as a metrazole antagonist, consistent with its relatively low affinity and partial agonist properties in the TBPS and chloride current assays. Both of these analogs were significantly less potent in this *in vivo* assay than **2** (ED_{50} = 1.6 mg/kg), which is remarkably active given that it is an antagonist by *in vitro* determinants.

Further exploration of this series with substituents at the 6- and 7-positions provided some intriguing results. Substitution at the 6-position had profound effects on affinity and *in vitro* efficacy. In particular, 6-chloro **38** had an 8-fold improvement in affinity (K_i = 14.6 nM) as compared to **27** (K_i of 115 nM). By the TBPS assay this compound was 2 times as efficacious

Table 2. Physical Data for Imidazo[1,5-*a*]quinoxaline Ureas, Carbamates, and Amides

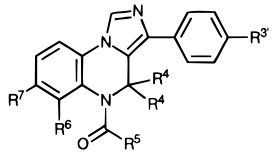

compd	$R^{3'}$	R^4	R^5	R^6	R^7	mp (°C)	method	yield (%)	formula	anal.
41	H	H	NMe_2	H	H	225−226	C	39	$C_{19}H_{18}N_4O\cdot(H_2O)_{1/5}$	C, H, N
42	F	H	NMe_2	H	H	192−193.5	E	74	$C_{19}H_{17}N_4OF$	C, H, N
43	Me	H	NMe_2	H	H	204−205	E	52	$C_{20}H_{20}N_4O$	C, H, N
44	H	H	pyrrolidine	H	H	205−207	C	37	$C_{21}H_{20}N_4O$	C, H, N
45	F	H	pyrrolidine	H	H	217−218	E	72	$C_{21}H_{19}N_4OF$	C, H, N
46	Me	H	pyrrolidine	H	H	238.5−239.5	E	81	$C_{22}H_{22}N_4O$	C, H, N
47	F	H	morpholine	H	H	193−194	E	76	$C_{21}H_{19}N_4O_2F$	C, H, N
48	F	H	3,5-dimethylpiperazine	H	H	207−209	E	87	$C_{23}H_{24}N_5OF\cdot(H_2O)_{1/4}$	C, H, N
49	F	H	3,4,5-trimethylpiperazine	H	H	167−169	G	57	$C_{24}H_{26}N_5OF\cdot(H_2O)_{1/4}$	C, H, N
50	H	H	piperidine	H	H	177−180	C	35	$C_{22}H_{22}N_4O\cdot(H_2O)_{1/4}$	C, H, N
51	F	H	NH_2	H	H	222−223	E	63	$C_{17}H_{13}N_4OF$	C, H, N
52	F	H	NHEt	H	H	196−200	E	86	$C_{19}H_{17}N_4OF$	C, H, N
53	F	H	NHtBu	H	H	241−243.5	C	40	$C_{21}H_{21}N_4OF$	C, H, N
54	H	Me	NMe_2	H	H	224−225.5	B	74	$C_{21}H_{22}N_4O$	C,[a] H, N
55	F	Me	NMe_2	H	H	248−249	B	55	$C_{21}H_{21}N_4OF$	C, H, N
56	Me	Me	NMe_2	H	H	248−249	B	23	$C_{22}H_{24}N_4O$	C, H, N
57	F	Me	pyrrolidine	H	H	232−233	B	48	$C_{23}H_{23}N_4OF$	C, H, N
58	Me	Me	pyrrolidine	H	H	215−216	B	31	$C_{24}H_{26}N_4O$	C, H, N
59	F	H	OMe	H	H	156−160	D	35	$C_{18}H_{14}N_3O_2F$	C, H, N
60	F	H	OiPr	H	H	160−160.5	D	42	$C_{20}H_{18}N_3O_2F$	C, H, N
61	F	H	*p*-F-Ph	H	H	230−231	F	72	$C_{23}H_{15}N_3OF_2$	C, H, N
62	F	H	*m*-F-Ph	H	H	176−177	F	75	$C_{23}H_{15}N_3OF_2$	C, H, N
63	F	H	*o*-F-Ph	H	H	185−189	F	78	$C_{23}H_{15}N_3OF_2$	C, H, N
64	F	H	morpholine	H	F	180−181.5	E	75	$C_{21}H_{18}N_4F_2O_2$	C, H, N
65	F	H	morpholine	H	Cl	142−144	E	48	$C_{21}H_{18}N_4O_2ClF$	C, H, N, Cl
66	F	H	morpholine	Cl	H	280−281	C	42	$C_{21}H_{18}N_4O_2ClF$	C, H, N, Cl
67	F	H	3,5-dimethylpiperazine	H	F	139−141	E	37	$C_{23}H_{23}N_5F_2O\cdot(H_2O)_{1/4}$	C, H, N
68	F	H	3,4,5-trimethylpiperazine	H	F	112−114	G	78	$C_{24}H_{25}N_5F_2O\cdot(H_2O)_{1/2}$	C, H, N
69	F	H	3,5-dimethylpiperazine	Cl	H	203−205	C	64	$C_{23}H_{23}N_5OClF$	C, H, N, Cl
70	F	H	3,4,5-trimethylpiperazine	Cl	H	213−214	G	81	$C_{24}H_{25}N_5OClF$	C,[b] H, N, Cl
71	OMe	H	3,5-dimethylpiperazine	H	H	184−185	E	47	$C_{24}H_{27}N_5O_2\cdot(H_2O)_{1/2}$	C, H, N
72	OMe	H	3,4,5-trimethylpiperazine	H	H	177.5−180	G	49	$C_{25}H_{29}N_5O_2\cdot(H_2O)_{1/4}$	C, H, N

[a] C: calcd, 72.81; found, 73.22. [b] C: calcd, 63.50; found, 62.42.

as diazepam, while the close analog **37** (*p*-OMe) was a full agonist (TBPS shift of 1.0). Most fascinating was that **38** had 7-fold greater efficacy than diazepam in the chloride current assay ($\alpha_1\beta_2\gamma_2$ subtype), while **37** was also a potent agonist. This degree of efficacy has not been previously observed in any of the other classes of BzR ligands that we have studied. Both of these compounds were extremely effective in the metrazole antagonism assay. Interestingly, **37** and the two 6-methyl-analogs, **39** and **40**, did not have enhanced binding affinity over the unsubstituted analogs **24** and **27**. Nonetheless, both of the 6-methylquinoxalin-4-ones (like the 6-chloro derivatives) were full agonists, having up to 3-fold greater efficacy than diazepam in the chloride current assay ($\alpha_1\beta_2\gamma_2$ subtype), and were potent metrazole antagonists. The dramatic improvement in affinity and efficacy through 6-chloro substitution (i.e., **38**) is unique and in clear contrast to classical benzodiazepine SAR.[10,11] In contrast, substitution at the 7-position with a chloro group (**36**) resulted in dramatically decreased affinity (15-fold lower than **27**) yet had little effect on *in vitro* efficacy. The 7-fluoro analogs as a group were also quite different. While **33** had similar affinity to **23**, **34** suffered a 2-fold decrease in affinity over unsubstituted **24**. The contrast was true for the **35** and **27** pair, with **35** having 2-fold greater affinity. While all three of the 7-fluoro analogs had greater *in vitro* efficacy as compared to the unsubstituted analogs, none were active in the metrazole antagonism assay.

The disparate values between the TBPS shift and Cl^- current assays for several of these compounds may, in part, be attributed to heterogeneity of the $GABA_A$ receptor population. Classical benzodiazepines interact with the $\alpha_1\beta_2\gamma_2$, $\alpha_2\beta_2\gamma_2$, $\alpha_3\beta_2\gamma_2$, and $\alpha_5\beta_2\gamma_2$ subtypes with nearly equal affinity,[21] while atypical BzR ligands such as CL 218872 and Zolpidem have moderate selectivity for the $\alpha_1\beta_2\gamma_2$ subtype.[4a,21] However, classical benzodiazepines do not interact with the $\alpha_6\beta_2\gamma_2$ subtype located in cerebellar granule cells, whereas ligands such as Ro 15-4513 have high affinity for this subtype.[22] Furthermore, these BzR ligands often display efficacy selectivity where Cl^- current is modulated to varying degrees in these receptor subtypes.[23] The search for selective ligands for these subtypes as well as the elucidation of their function remains an important goal in this area.

A few analogs from this series were examined in two different benzodiazepine receptor subtypes.[24,25] Binding affinity for a number of compounds from this series was measured in the $\alpha_1\beta_2\gamma_2$ and $\alpha_3\beta_2\gamma_2$ receptor subtypes with little selectivity noted. The only compound displaying modest selectivity (4-fold) was **38**, which had a K_i of 17 nM in $\alpha_1\beta_2\gamma_2$ and a K_i of 72 nM in $\alpha_3\beta_2\gamma_2$. The rest of the analogs evaluated had essentially equivalent

Table 3. [^{3}H]Fnz Binding, TBPS Shift, Cl^- Current Changes, and Metrazole Antagonism Data for Imidazo[1,5-*a*]quinoxalin-4-ones

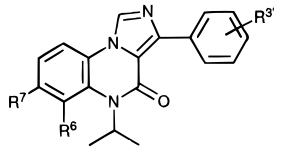

compd	$R^{3'}$	R^6	R^7	K_i (nM)[a]	[^{35}S]TBPS shift[b,c]	Cl^- current[b,c] $\alpha_1\beta_2\gamma_2$	Cl^- current[b,c] $\alpha_3\beta_2\gamma_2$	metrazole[d] ED_{50} (mg/kg, ip)
23	H	H	H	38.5	0.31	0.07		>50
24	4′-OCH_3	H	H	31.7	0.75	0.45		12.5
25	4′-CH_3	H	H	174	1.09	0.38		>50
26	4′-Cl	H	H	2890	0.74	0.04		>50
27	4′-F	H	H	115	0.58	0.43	0.45	30
28	4′-CF_3	H	H	>10000	0.36	1.02	0.36	
29	3′-OCH_3	H	H	207	0.24	1.0	0.12	>50
30	3′-F	H	H	480	0.31	0.11		>50
31	3′-CF_3	H	H	188	0.45	0.44	0.03	>50
32	2′-OCH_3	H	H	>10000		>50		
33	H	H	F	39.6	0.77	0.50		>50
34	4′-OCH_3	H	F	81.5	0.97	1.05		>50
35	4′-F	H	F	59.4	0.80	0.72		>50
36	4′-F	H	Cl	1692	0.14	0.36	0.03	>50
37	4′-OCH_3	Cl	H	27.9	1.04	2.23	1.0	1.3 (1.0−1.9)
38	4′-F	Cl	H	14.6	2.04	7.0	3.4	0.9 (0.7−1.3
39	4′-OCH_3	CH_3	H	49.7	0.92	1.8	1.3	3.1 (1.7−5.8)
40	4′-F	CH_3	H	126	1.83	3.2	1.7	2.6 (1.9−3.7)
diazepam				4.9	1.0 ± 0.2	1.0 ± 0.2	1.0 ± 0.2	0.50 (0.38−1.2)
2				1.6	0.06	0.04		1.6

[a] Mean binding affinity against [^{3}H]flunitrazepam; see ref 15 and the Experimental Section for methods. The standard error was <±10% of the mean. [b] Diazepam is defined as a full agonist which gives a value of 1. Antagonists are defined as having a shift value of 0; partial agonists are intermediate. [c] See the Experimental Section. The standard error was <±10% of the mean. [d] Antagonism of metrazole-induced clonic convulsions in the rat after ip injection; see the Experimental Section.

affinity for each subtype. However, significant differences in efficacy in the Cl^- current assay were noted for most of the 3-phenyl quinoxalin-4-ones evaluated in these two subtypes. All but one of the analogs evaluated (**27**) had enhanced efficacy in the $\alpha_1\beta_2\gamma_2$ subtype (data provided in Table 3). Most notably, **29** was a full agonist in $\alpha_1\beta_2\gamma_2$ while an antagonist in the $\alpha_3\beta_2\gamma_2$ subtype. For some of the more agonistic analogs, efficacy was up to 2-fold greater in the $\alpha_1\beta_2\gamma_2$ subtype.

In contrast to the quinoxalin-4-one series and the imidazobenzodiazepine literature, the replacement of the oxadiazole group with a phenyl substituent in the quinoxaline urea class (dimethyl, pyrrolidino, morpholino) maintained excellent binding affinity as indicated for analogs **41**−**47** in Table 4. Comparison of **41** to **1** indicates only a 3-fold loss of affinity (3.4 vs 1.0 nM), while pyrrolidine urea analogs with a 3-phenyl (**44**) or 3-oxadiazole[6b] substituent have nearly identical affinity. Fluoro and methyl substituents at the *para*-position of the 3-aryl ring were also well tolerated with only **43** suffering a slight loss of affinity as compared to **41**. Like **1**, most of these urea analogs were partial agonists as indicated by their TBPS shift ratios. The only exception was full agonist **46** which contained a 4′-methyl substituent. Most of these analogs were also partial agonists in the chloride current assay which was run only in the $\alpha_1\beta_2\gamma_2$ subtype. Again *p*-methyl substitution provided for enhanced efficacy, in the general order Me > F > H for the pyrrolidine analogs. The morpholine analog **47** was also a full agonist by Cl^- current measurement, consistent with its exceptional activity in the metrazole antagonism assay. The other analogs examined in this assay were also quite effective at antagonizing metrazole-induced seizures, substantially more potent than **1**. From this brief SAR study, the 4′-fluorophenyl substituent provided the most desirable profile (high affinity/partial agonist) and was used for further analog development.

Quite a few additional substituents were explored at the 5-position. Primary and monoalkyl ureas **51**−**53** had surprisingly low affinity (49−283 nM) as did the two carbamate analogs **59** and **60**, in marked contrast to the oxadiazole series.[6b] These analogs were partial to full agonists as determined by the TBPS shift and chloride current assays but, other than the potent agonist **60**, were inactive in the metrazole antagonism assay. The isopropoxy derivative **60**, like other carbamates in the oxadiazole series,[6] had 2-fold greater efficacy than diazepam in the Cl^- current screen. Of the three benzamide analogs, only **62** had reasonable affinity with a K_i of 5.9 nM. The fluoro groups on the benzamide substituent had a fairly dramatic and unexpected effect on both *in vitro* and *in vivo* efficacy, with **62** having almost a 3-fold greater enhancement of chloride current than diazepam. This compound was also extremely effective in the metrazole antagonism assay in contrast to **61**, presumably due to increased *in vitro* efficacy and affinity.

In light of the desirable profile of selected compounds such as **42** and **45**, other dialkyl urea substituents were examined at the 5-position. A piperidine ring (**50**) was also tolerated having similar affinity and efficacy (TBPS) to **47**. However, by chloride current measurement, the piperidine analog was a partial agonist having about one-half the efficacy of **47** and was about 10-fold less potent in the metrazole antagonism assay. Quite surprisingly, the relatively bulky *cis*-3,5-dimethylpiperazine and *cis*-3,4,5-trimethylpiperazine groups could also be incorporated into this template with high affinity maintained. These piperazines were incorporated into

Table 4. [^{3}H]Fnz Binding, TBPS Shift, Cl^- Current Changes, and Metrazole Antagonism Data for Imidazo[1,5-*a*]quinoxaline Ureas, Carbamates, and Amides

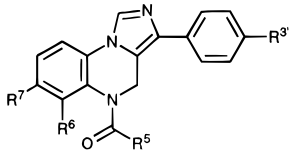

compd	$R^{3'}$	R^5	R^6	R^7	K_i (nM)[a]	[^{35}S]TBPS shift[b,c]	Cl^- current,[b,c] $\alpha_1\beta_2\gamma_2$	metrazole[d] ED_{50} (mg/kg, ip)
41	H	NMe_2	H	H	3.41	0.40	0.36	
42	F	NMe_2	H	H	2.96	0.53	0.68	4.4 (2.7−7.2)
43	Me	NMe_2	H	H	11.1			4.4 (2.6−7.7)
44	H	pyrrolidine	H	H	0.37	0.69	0.52	
45	F	pyrrolidine	H	H	0.97	0.64	0.85	14.8 (8.8−25)
46	Me	pyrrolidine	H	H	1.54	1.19	1.08	
47	F	morpholine	H	H	1.61	0.54	1.07	0.30
48	F	3,5-dimethylpiperazine	H	H	5.85	0.75	0.89	1.1 (1.1−1.1)
49	F	3,4,5-trimethylpiperazine	H	H	13.2	0.31	0.56	13 (8.4−18.5)
50	H	piperidine	H	H	1.65	0.52	0.52	4.5 (2.3−8.8)
51	F	NH_2	H	H	216	0.29	0.69	>50
52	F	NHEt	H	H	48.6	0.42	1.00	>50
53	F	NHtBu	H	H	283	1.02	1.00	>50
54[e]	H	NMe_2	H	H	478	0.45	0.27	
55[e]	F	NMe_2	H	H	163	0.49	0.38	>50
56[e]	Me	NMe_2	H	H	334	0.71	0.80	>50
57[e]	F	pyrrolidine	H	H	12.6	0.60	0.54	>50
58[e]	Me	pyrrolidine	H	H	35.0	1.05	0.81	17.7 (17.7−17.7)
59	F	OMe	H	H	47.2	0.53	0.21	>50
60	F	OiPr	H	H	50.8	0.93	2.0	6.3 (3.9−10.1)
61	F	*p*-F-Ph	H	H	20.5	0.82	0.48	29.7 (17.7−50)
62	F	*m*-F-Ph	H	H	5.91	1.06	2.75	1.3
63	F	*o*-F-Ph	H	H	42.4	0.84	0.80	
64	F	morpholine	H	F	2.16	0.70	0.58	0.14 (0.08−0.26)
65	F	morpholine	H	Cl	15.2	1.05	0.78	0.76 (0.44−1.30)
66	F	morpholine	Cl	H	2.97	0.44	1.09	3.7 (1.9−7.6)
67	F	3,5-dimethylpiperazine	H	F	2.49	0.72	1.17	0.5 (0.35−0.91)
68	F	3,4,5-trimethylpiperazine	H	F	5.06	0.64	1.25	1.3 (1.0−1.9)
69	F	3,5-dimethylpiperazine	Cl	H	33.4	0.31	0.93	1.8 (1.13−3.14)
70	F	3,4,5-trimethylpiperazine	Cl	H	47.4	0.62	1.12	1.8 (1.13−3.14)
71	OMe	3,5-dimethylpiperazine	H	H	1.39	0.31	1.09	0.8 (0.5−1.2)
72	OMe	3,4,5-trimethylpiperazine	H	H	4.16	0.27	0.87	0.8 (0.4−1.5)
1					1.0	0.69	0.68	21

[a] Mean binding affinity against [^{3}H]flunitrazepam; see ref 15 and the Experimental Section for methods. The standard error was <±10% of the mean. [b] Diazepam is defined as a full agonist which gives a value of 1. Antagonists are defined as having a shift value of 0; partial agonists are intermediate. [c] See the Experimental Section. The standard error was <±10% of the mean. [d] Antagonism of metrazole-induced clonic convulsions in the rat after ip injection; see the Experimental Section. [e] *gem*-4,4-Dimethyl substitution.

this template as work in the related 3-*tert*-butyl ester series revealed that considerably improved *ex vivo* binding and pharmacokinetic properties result for this substitution (*vide infra*).[26] Both **48** and **49** suffered only a 5−10-fold decrease in affinity (K_i = 5.8 and 13.2 nM, respectively) as compared to **47** or **50**. Trimethylpiperazine **49** was a partial agonist by both TBPS shift and chloride current measurements with corresponding activity in the metrazole antagonism assay. The dimethyl analog had greater *in vitro* efficacy (TBPS 0.75; Cl^- current 0.89) and was extremely effective as a metrazole antagonist (ED_{50} = 1.1 mg/kg). To modulate efficacy, the *para*-substituent on the 3-aryl ring was also varied to include a methoxy group within the piperazine urea framework. Both analogs **71** and **72** had high affinity and were weak partial agonists by TBPS shift determination. Interestingly, by chloride current measurement, both urea analogs were full agonists with exceptional potency in the metrazole assay.

In contrast to the high binding affinity observed for most analogs within this series, ureas containing *gem*-dimethyl substitution at the 4-position were disappointing. For the dimethylamino ureas, the *gem*-dimethyl analogs suffered between a 30- and 140-fold drop in affinity. This substitution pattern combined with a pyrrolidine urea led to an improvement in affinity with **57** having a K_i of 12.6 nM. The low affinity observed for many of these analogs is quite surprising as the corresponding oxadiazole derivatives[6b] had K_i's of roughly 3 nM. These urea analogs were all partial agonists except for **58**, which was a full agonist as indicated by its TBPS shift ratio and, nearly so, as determined by chloride current measurement. Only **58** was active as a metrazole antagonist.

The role of chloro and fluoro groups at the 6- and 7-positions on *in vitro* and *in vivo* activity was also examined in the quinoxaline series. The urea groups were maintained as either a morpholine, *cis*-3,5-dimethylpiperazine, or *cis*-3,4,5-trimethylpiperazine. In the 6-chloro series the morpholine analog **66** had similar affinity and *in vitro* efficacy to **47**. The metrazole activity, however, was decreased by roughly 12-fold. The two piperazine analogs **69** and **70** were less tolerant of this substitution with affinity notably decreased. Nonetheless, both analogs had similar or enhanced efficacy over **48** and **49** in the TBPS shift and chloride current assays. Both of the 6-chloro analogs were also extremely effective in the metrazole antagonism assay (ED_{50} = 1.8 mg/kg), which is surprising given their affinity and the decreased activity of **66** as compared

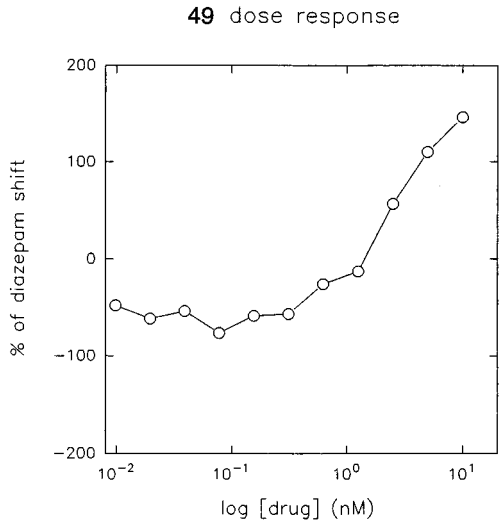

Figure 2. Cl^- current dose−response curve of **49**. Full agonist = −100, antagonist = 0, full inverse agonist = +100.

to **47**. In the 7-chloro series only the morpholine analog **65** was synthesized. This derivative had decreased affinity as compared to **47**. The TBPS shift ratio was notably increased for **65**, while the chloride current was lower. Even with decreased affinity, **65** was quite effective in the metrazole antagonism assay. Substitution with a 7-fluoro group maintained (for morpholine) or enhanced (for **67** and **68**) binding affinity as compared to the unsubstituted analogs. The TBPS shift ratio is consistent with the three fluoro analogs as being partial agonists, while by chloride current determination, the piperazine analogs **67** and **68** were full agonists. All three urea analogs were quite potent in the metrazole assay. Overall, substitution with a chloro group at the 6- or 7-position or with a 7-fluoro often resulted in decreased affinity with mixed effects on *in vitro* efficacy. Frequently the chloride current was increased for the halogenated analogs, while metrazole activity was usually maintained or enhanced. In marked contrast, halogenated analogs in the oxadiazole series were devoid of metrazole activity.[6b] The dramatic effects of 6-Cl substitution observed in the 3-phenyl quinoxalin-4-one series were absent in this class. Evaluation of selected members of this class for affinity and efficacy in the $\alpha_1\beta_2\gamma_2$ and $\alpha_3\beta_2\gamma_2$ subtypes revealed little selectivity. Of the compounds screened, only **66** displayed modest selectivity (6-fold) for the $\alpha_1\beta_2\gamma_2$ subtype (K_i = 1.6 vs 9.5 nM), while no analogs exhibited differential efficacy between these subtypes.

Within the quinoxaline urea series, the values for Cl^- current and the TBPS shift ratio were consistently quite different, with greater efficacy usually indicated by the chloride current screen. While this is often the case as the chloride current assay was usually determined in only a single receptor subtype ($\alpha_1\beta_2\gamma_2$), whereas the TBPS shift ratio was measured across all native receptors as mentioned previously, the frequent discrepancy between these values (particularly for the piperazines) was intriguing. Further investigation of this subclass revealed that the differences between these assays may, in part, be explained due to a biphasic dose−response curve observed for the piperazine analogs in both of these assays. The dose−response curve for chloride current ($\alpha_1\beta_2\gamma_2$ subtype) of **49**, which is typical of the piperazine class, is shown in Figure 2. As apparent, at

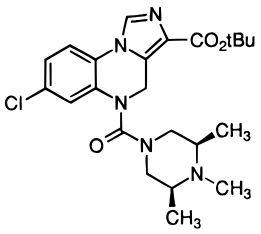

73 (U-97775)

Figure 3. Piperazinyl quinoxaline **73**.

low concentrations **49** is nearly a full agonist (−90). However with increasing concentration, the Cl^- current decreases to 0% of diazepam, consistent with antagonistic properties. At even higher concentrations, **49** behaves as an inverse agonist (>+100). The TBPS shift ratio was also found to have a dose-dependent relationship (data not shown). The different values reported for the two screening assays (Table 4) for analogs in the piperazine class may thus be a reflection of different concentrations used for the test substance as the TBPS assay was run at 5.0 μM whereas Cl^- current was measured at 0.5 μM.

Biphasic effects in the *in vitro* assays were only observed for the piperazine ureas. Compounds with other substituents at the 5-position, or the imidazo[1,5-*a*]quinoxalin-4-ones, did not express biphasic properties. Interestingly, the substituent at the 3-position may be modified within the quinoxaline piperazine framework to include oxadiazoles, *tert*-butyl esters,[26] and isoxazoles with the biphasic dose−response curve maintained. As reported for *tert*-butyl ester analog **73** (U-97775; Figure 3), the unique biphasic effects observed for these piperazines is most likely the result of these compounds having two distinct binding sites on the $GABA_A$ complex, a high-affinity site and a low-affinity site.[27] To our knowledge, the biphasic properties observed for these piperazines are unique and have not been observed for other classes of BzR ligands. Frequently, the reverse situation does occur with the degree of agonism increasing with drug concentration. Therapeutically, compounds such as **49** could be quite unique among BzR ligands as their agonistic properties would presumably be limited across a wide dose range, if the *in vivo* activity parallels the *in vitro* properties. In particular, drug abuse problems, which are common for BzR ligands, may be lessened for these agents.

On the basis of the results of the *in vitro* (binding, TBPS shift, Cl^- current) and metrazole assays, selected compounds from both series were evaluated for typical benzodiazepine-type side effects. As with the oxadiazole series,[6] two of the most important side effects promoted by BZD full agonists are ethanol potentiation and physical dependence. The potentiation of the effects of alcohol by the test compounds was determined by measuring the drug ED_{50}s for traction and loss of righting after coadministration. In this assay,[6b] diazepam had ED_{50}'s of 0.54 and 0.86 mg/kg for traction and loss of righting reflex, respectively. The degree of acute physical dependence was assessed through an electroshock seizure assay.[28a] Withdrawal from chronic high-dose treatment of benzodiazepines may in some cases result in signs and symptoms related to hyperexcitability of the CNS. Clinically, these manifestations of physical dependence are undesirable as they are

Table 5. Benzodiazepine Antagonism, Ethanol Potentiation, and Acute Physical Dependence Data for Imidazo[1,5-*a*]quinoxalines

compd	BZD antag traction[a] ED_{50} (95% confidence interval) (mg/kg)	ethanol potentiation ED_{50} (95% confidence interval) (mg/kg)		acute electroshock physical dependence activity[b,c] (drug MA_{50}/ V122 MA_{50})
		traction[a]	LRR	
24		>30	>30	
27	>30	14 (7−28)	>30	IA (20.9/20.9)
37	>30	>30	>30	IA (19.3/21.2)
38				A (15.0/21.9)
39	>30			A (17.7/19.5)
40	>30			A (15.4/19.7)
42	4.9 (2−9)	11 (6−19)	>30	A (15.9/18.1)
43				A (16.9/19.4)
45	>30	0.34 (0.19−0.61)	>30	A (17.9/20.3)
47				A (13.9/20.7)
48	>30	4.0 (2−9)	>30	A (12.5/17.7)
49	>30			A (16.5/20.5)
50	>30	0.5 (0.2−1.0)	>30	A (14.9/18.1)
60	>30	>30	>30	A (17.7/21.1)
62				A (18.1/20.7)
64	>30	5 (3−10)	17 (17−17)	A (14.8/21.1)
65	>30	11 (6−19)	27 (15−49)	A (12.1/19.4)
66				A (17.0/19.7)
67	>30			
68				A (12.4/21.0)
69	>30			
70	>30			A (15.7/19.5)
71	>30			A (9.4/19.7)
72	>30			A (11.9/19.7)
diazepam		0.54 (0.54−0.54)	0.86 (0.5−1.4)	A[d] (18.2/25.4)
2	1.7 (0.8−3.8)	6.6 (3.3−13)	>30	IA (21.2/22.2)
1	1	27	>30	IA (23.2/24.9)

[a] See the Experimental Section. [b] $p < 0.05$; IA no significant activity. [c] See the Experimental Section. [d] Tested at 15 mg/kg.

similar to the disorder being treated.[28b] Furthermore, the abuse potential for drugs inducing physical dependence generally leads to scheduling of the compound by the regulatory agencies. With this in mind, it is highly desirable that new benzodiazepine-related therapeutic agents under development have minimized physical dependence-inducing properties. In animals, changes in hyperexcitability can be quantified by determining the current seizure threshold (MA_{50}) to elicit electroshock-induced seizures. In this assay, the lowering of electroshock thresholds precipitated by a benzodiazepine antagonist after an acute regimen of test compound was used to quantify the development of physical dependence. Mice having received either drug or vehicle were assessed for electroshock seizure thresholds (drug MA_{50} compared to vehicle MA_{50}) 5 min after flumazenil-precipitated withdrawal. Diazepam was active at doses as low as 15 mg/kg/day in this assay. In contrast, both **1** and **2** did not produce physical dependence at doses up to 150 mg/kg/day. In the alcohol enhancement screen, only **2** promoted traction (ED_{50} = 6.6 mg/kg) with no effects on loss of righting observed for either compound. Finally, while not a direct measure of a benzodiazepine-type side effect, many of the analogs were evaluated for their ability to antagonize the muscle relaxation effects of triazolam, a full agonist BzR ligand. Diazepam and related full agonist benzodiazepines were inactive in this assay, whereas partial agonists such as **1** and **2** were quite effective, with ED_{50}'s of 1.0 and 1.7 mg/kg, respectively.

Even though many of the quinoxalines had low efficacy in the TBPS and Cl^- current assays, consistent with antagonist or partial agonist profiles, only one compound **42** (ED_{50} = 4.0 mg/kg) was active as a benzodiazepine antagonist in the *in vivo* assay (Table 5). These results are quite surprising as many of the corresponding oxadiazole analogs, which had similar *in vitro* activity, were effective triazolam antagonists.[6b] In the ethanol potentiation screen, most analogs did not have significant effects on the loss of righting reflex, with only **64** and **65** weakly active. Like **2** and several compounds from the series derived from **1**, a number of analogs had significant effects on traction. Quinoxaline ureas **45** and **50** were quite potent with ED_{50}'s similar to that of diazepam, although neither of these derivatives were full agonists by the TBPS shift and Cl^- current screens. Of the five quinoxalin-4-ones tested in the acute physical dependence screen, only **27** and **37** were inactive. The lack of activity of **27** in this side effect screen is consistent with its *in vitro* behavior (low-efficacy partial agonist) in contrast to **37**, which would be expected to be active due to its full agonist properties. The other three analogs within this series were active in the electroshock assay, consistent with their "super" agonist *in vitro* profile. Unfortunately, all of the 3-phenylquinoxaline urea analogs of **1** were active in the acute physical dependence screen.

The potent activity observed in the acute physical dependence assay across the quinoxaline urea series is completely unexpected considering that many of these phenyl derivatives have *in vitro* properties consistent with that of a partial agonist, like the corresponding oxadiazole analogs, which often did not produce physical dependence. Furthermore, several analogs had exceedingly low electroshock seizure thresholds, lower than that produced by diazepam, albeit at 10 times the dose (150 mg/kg for the test compound as compared to 15 mg/kg diazepam). The most efficacious compounds in this side effect assay contained either piperazines or morpholine urea groups at the 5-position. Additionally, an electron-donating substituent (OMe) at the *para*-position of the 3-phenyl ring had significant effects on

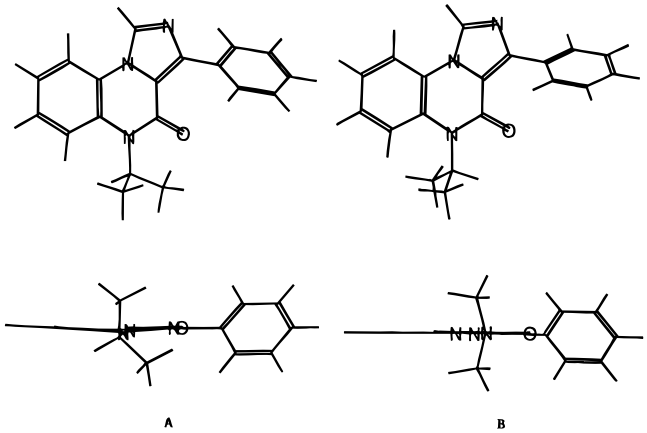

Figure 4. Molecular structures of the two lowest-energy conformers of **23**.

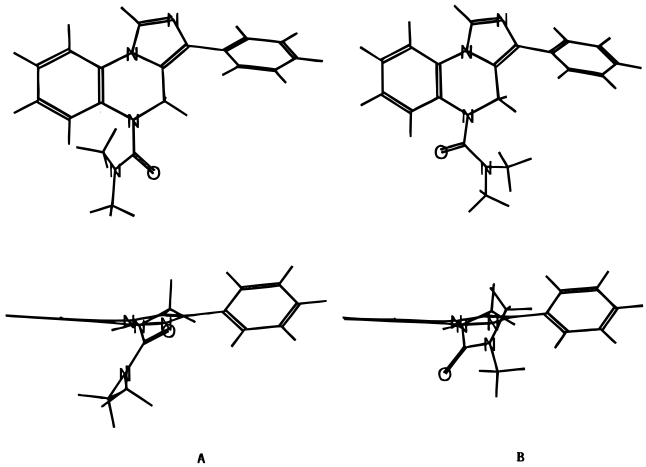

Figure 5. Molecular structures of the two lowest-energy conformers of **41**.

activity with **71** and **72** having the lowest electroshock potentials after drug withdrawal. The oxadiazole analog of **47** was active in this assay[6b] but had a significantly greater seizure threshold: 86% of control vs 67% of control for **47**. Similarly, the oxadiazole analogs containing piperazine ureas were also active but again had significantly higher seizure threshold values (83% of control). These results suggest that the high degree of activity of these piperazines (and morpholines) in the acute physical dependence assay is not directly related to their biphasic properties. Instead, the potent effects of the 3-phenylquinoxaline ureas in the physical dependence assay as compared to the oxadiazole analogs are consistent with the 3-phenyl group promoting this side effect. The reasons for the remarkable differences between the phenyl and oxadiazole series in this assay are unclear but may relate to changes in the binding interactions of the 3-substituent, subtype selectivity, metabolism, or CNS penetration.

Molecular Conformations. The low-energy conformers of a number of the present analogs were determined by molecular mechanics methods. Calculations were performed with both the AMBER* and MM2* force fields, which were developed for the MacroModel[29] system of programs as extensions of the original AMBER[30] and MM2[31] parameter sets. For each analog, 200 initial structures were generated using an internal coordinate Monte Carlo procedure[32] in which torsional angles around all rotatable bonds were allowed to vary. Subsequently, each initial structure was subjected to energy minimization, and duplicate minimized structures were discarded in compiling the final set of conformers. It should be noted that at each relative energy minimum, a pair of mirror image conformers was obtained, only one of which is described below.

In studies of the quinoxalin-4-one series of compounds, both the AMBER* and MM2* force fields gave essentially the same structures and relative energies, and thus only data obtained using the AMBER* force field are discussed below. Figure 4 shows the two lowest-energy conformers of **23**, structure A being more stable than B by only 0.67 kcal/mol. The two structures, which are typical of most analogs in this series, are identical except for the orientation of the isopropyl group, which in structure B is rotated 150° relative to that in structure A, as shown. The 3-phenyl group is not coplanar with the imidazoquinoxaline substructure; instead it may assume one of two possible minimum-energy orientations corresponding to out-of-plane rotations of ±50°.

For the imidazoquinoxaline urea template, calculations using the AMBER* and MM2* force fields yielded very similar structures but differing energetics. Figure 5 shows the two lowest-energy conformers of **41** obtained using the AMBER* force field. Structures A and B are identical except for the orientation of the 5-substituent. The 3-phenyl group is rotated 30° out-of-plane, with the edge of the phenyl ring nearer to N_2 located below the plane. With the exception of the 3-substituent, structures A and B of **41** are identical with those of the oxadiazole analog **1**.[6b] For the *gem*-dimethyl analog **54**, two low-energy conformers with imidazoquinoxaline rings and 5-substituents similar to those shown in Figure 5 were obtained. However, the 3-phenyl group in both conformers of **54** was constrained to lie approximately perpendicular to the plane.

Relative energies calculated for **41** and **54** followed the same trends obtained previously for other imidazoquinoxalines.[6b] Specifically for **41**, structure B was more stable than A by 0.74 kcal/mol according to the AMBER* calculations, but the reverse order and a larger energy difference of 3.38 kcal/mol was obtained using MM2*. Therefore, the preferred conformation of **41** and related analogs could not be determined from the present methods. In the case of **54**, both approaches predicted structure A to be more stable than B, with energy differences of 2.89 and 6.29 kcal/mol from AMBER* and MM2*, respectively.

Pharmacophore Models. As discussed in a previous report,[6b] the imidazoquinoxaline series of BzR ligands exhibit a number of features consistent with general models of BzR recognition and activation proposed by Wermuth et al.[33] and Gardner.[34] In particular, the fused phenyl component of the quinoxaline ring and the N_2 atom act as the aromatic region and hydrogen-acceptor site (δ_1), respectively, regarded as two important features necessary for receptor recognition.[33,34] Furthermore, in the quinoxalin-4-one series, the C_4-carbonyl group may correspond to a second hydrogen-acceptor site (δ_2) described in models developed by Villar[35] and Cook,[36] and also included in the Wermuth model. However, the $\delta_1-\delta_2$ distance of 4.2−4.4 Å in **23** and related analogs is somewhat longer than the range of 3.0−3.5 Å specified in the Villar model. In the

quinoxaline urea series, there is no substituent that correlates to the δ_2 site in these models.[6b]

The R^5 substituent corresponds to the "out-of-plane" region described by Wermuth, which is believed to correlate with full agonist activity.[33] In the present study, this region appears to be particularly effective in enhancing efficacy when R^5 is an isopropyl group forced into an out-of-plane position as in the 6-substituted analogs **38** and **40**. Similar effects have been reported previously for the **2** series of analogs as well.[7b] Furthermore, bulky R^5 substituents in this out-of-plane region in the quinoxaline urea series were generally found to increase efficacy.[6b]

In the present imidazoquinoxalines, the 3-phenyl group correlates with both the "freely rotating aromatic" group in the Wermuth model and the ester group cited in the Gardner model. As shown by the present data, the choice of 3-substituent can have a major influence on binding affinity. The general trends in receptor affinity can be rationalized by examining the energy computed as a function of the rotation angle of the 3-substituent, as illustrated by the following discussion.

Energies were calculated by means of constrained molecular mechanics energy minimizations using the AMBER* force field. Each initial structure was constructed from the minimum-energy conformer by rotating the 3-substituent through a specific angle, ϕ; subsequently each structure was subjected to energy minimization using an additional torsional potential of sufficient strength to hold the 3-substituent in its initial orientation.

Figure 6 compares the energy of **2** as a function of ϕ with that of **23** and **32**. In **2**, the oxadiazole substituent is positioned 30° out of the imidazoquinoxaline plane in the minimum-energy structure and can easily be rotated into a planar position with the expenditure of only 0.65 kcal/mol. In contrast, the 3-phenyl substituent in **23** is seen to be confined to an out-of plane orientation (45−50°) and is not free to assume coplanarity with the imidazoquinoxaline ring. The phenyl ring though can be rotated to within 25−30° of planarity with only a modest energy expenditure (1.7−1.0 kcal/mol). Moreover, for **32**, an inactive compound, the 3-phenyl group may not be rotated to within 45° of planarity without both a substantial increase in energy and a significant distortion of the imidazoquinoxaline ring system.

Figure 7 shows a similar comparison for **1** and analogs **41** and **54**. The preferred orientation of the oxadiazole substituent in **1** is seen to be approximately planar, and out-of-plane geometries are increasingly unfavorable. In the minimum-energy structure of **41**, the 3-phenyl group is found with $\phi = 33°$, but it may be rotated to within 10° of planarity with a penalty of only 1 kcal/mol. Moreover, the 3-phenyl group in **41** may be freely rotated through a full 360° at a cost of no more than 2.70 kcal/mol. In contrast, the 3-phenyl group in the low-affinity *gem*-dimethyl analog **54** is clearly confined to a nonplanar conformation.

The preceding analysis shows that there is a clear correlation between binding affinity and the ability of the 3-substituent to assume a planar orientation at minimum-energy cost. This observation is consistent with the general tenets of the Wermuth and Gardner models and, in addition, provides a more precise statement of the conditions which must be placed on the 3-substituent to achieve high affinity at the BzR.

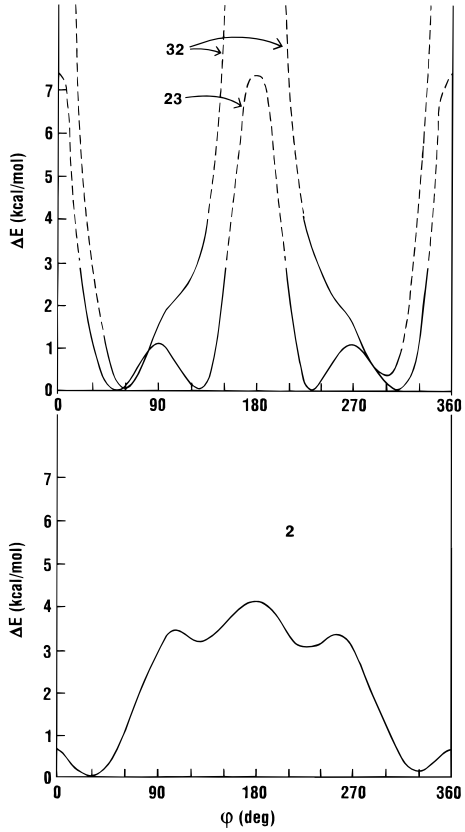

Figure 6. Relative energies (ΔE) of **2**, **23**, and **32** as a function of the rotation angle of the 3-substituent (ϕ). The value $\phi = 0$ corresponds to the 3-substituent positioned coplanar with the imidazole ring. Solid lines denote ranges of ϕ corresponding to free rotation of the 3-substituent with no additional distortions of the structure. Dashed lines indicate ranges of ϕ where restricted rotation and distortions of the imidazoquinoxaline ring were observed.

Conclusion

Substitution of the oxadiazole group for a phenyl ring at the 3-position in a series of imidazo[1,5-*a*]quinoxalin-4-ones invariably resulted in notably decreased binding affinity for the BzR. While *in vitro* efficacy was moderately enhanced for the phenyl analogs, anti-metrazole activity was dramatically decreased in comparison to the oxadiazole analogs. Uniquely, substitution at the 6-position with a chloro group resulted in significantly enhanced affinity and *in vitro* efficacy. Up to 7-fold greater efficacy than diazepam was noted for compound **38** in the Cl^- current assay, measured in cells expressing the $\alpha_1\beta_2\gamma_2$ subtype of $GABA_A$ receptors. Similar substitution with a methyl group at this position also led to highly efficacious compounds, although affinity was not increased. Most compounds from this series had greater efficacy in the $\alpha_1\beta_2\gamma_2$ subtype as compared to $\alpha_3\beta_2\gamma_2$, although little binding selectivity was observed.

In a related class of imidazo[1,5-*a*]quinoxaline ureas, replacement of the oxadiazole group by a phenyl ring usually maintained the high affinity typically observed in this series. The major exceptions proved to be compounds containing *gem*-dimethyl substituents at the 4-position. In both of these series, binding affinity correlated quite well with the ability of the 3-phenyl ring

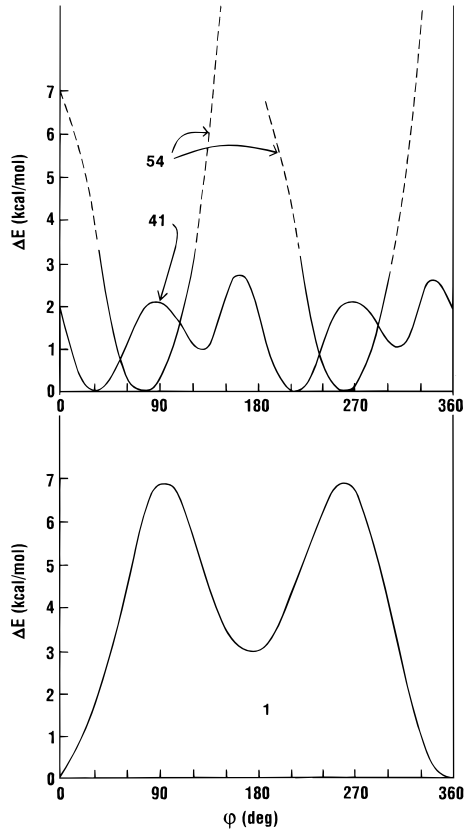

Figure 7. Relative energies (ΔE) of **1**, **41**, and **54** as a function of the rotation angle of the 3-substituent (ϕ). The conventions used in this figure are the same as those in Figure 6.

to rotate to near planarity to the imidazoquinoxaline ring system. Most of the urea analogs retained a partial agonist *in vitro* profile, regardless of the 3-phenyl substituent. The 5-position was widely tolerant of a number of functional groups (ureas, amides, carbamates) with relatively bulky substituents providing derivatives with good binding affinity. Compounds from this series did not display selectivity for the $\alpha_1\beta_2\gamma_2$ and $\alpha_3\beta_2\gamma_2$ subtypes (affinity, efficacy). Even with a partial agonist *in vitro* profile, many of the urea analogs displayed excellent activity in the metrazole antagonism assay. An unprecedented biphasic dose−efficacy relationship was noted for the piperazine urea subseries where, by *in vitro* measurement, the analogs became increasingly antagonistic with increasing drug concentration, theoretically limiting agonist-type properties at high dose levels. Unfortunately, almost all of the analogs from both series, which displayed anxiolytic-like activity in the *in vitro* and *in vivo* screening assays, produced an unacceptably high level of physical dependence in an acute electroshock assay, precluding further development.

Experimental Section

Chemistry. Thin-layer and flash chromatography utilized E. Merck silica gel (230−400 mesh). Melting points were taken on a Thomas-Hoover capillary melting point apparatus and are uncorrected. Mass spectra, infrared spectra, and combustion analysis were obtained by the Physical and Analytical Chemistry Department of The Upjohn Co. ^{1}H NMR spectra were recorded at 300 MHz with a Bruker Model AM-300 spectrometer.

In cases where synthetic intermediates or products were isolated by "aqueous workup (organic solvent, drying agent)," the procedure was to quench the reaction with H_2O, dilute with the indicated organic solvent, separate the organic layer, extract the aqueous layer several times with the organic solvent, dry the combined organic layers with the indicated drying agent, filter off the drying agent, and remove solvent using a rotary evaporator at reduced pressure. When "basic workup (organic solvent, aqueous basic solvent, drying agent)" is indicated, the procedure was similar to aqueous workup, except the indicated aqueous base was used instead of H_2O. When "acidic workup (organic solvent, organic solvent, drying agent)" is indicated, the procedure was to dilute the reaction mixture with the first indicated solvent, extract the organic solution several times with 10% HCl, basify the combined acidic layers with solid KOH, extract the basic solution with the second indicated organic solvent several times, dry the organic layers with the indicated drying agent, filter off the drying agent, and remove solvent using a rotary evaporator under reduced pressure. Tetrahydrofuran (THF) and ether were distilled from sodium and benzophenone. Dichloromethane was distilled from calcium hydride, and DMF was dried over 3 Å molecular sieves. All other solvents were EM Science HPLC grade, distilled in glass. Diethyl chlorophosphate and potassium *tert*-butoxide (1.0 M in THF) were purchased from the Aldrich Chemical Co., Milwaukee, WI. Phosgene in toluene (**CAUTION**: phosgene is highly toxic and should be used with extreme care) was purchased from Fluka Chemie AG or Columbia. All reactions were run under nitrogen or argon.

Preparation of 2,3-Dioxoquinoxaline Templates 5. *N*-Isopropyl-2-methyl-6-nitroaniline (12e). A mixture of 2-bromo-3-nitrotoluene (**11e**, Y = Br; 5.30 g, 24.5 mmol) and isopropylamine (30.0 mL) was heated at 150 °C in a bomb for 36 h. After cooling to room temperature the solution was concentrated. Basic workup (CH_2Cl_2, $NaHCO_3$, $MgSO_4$) gave 4.75 g (100%) of the product as an orange oil: IR (neat) 1605, 1533, 1485, 1451, 1339, 1325, 1264, 742 cm^{-1}; ^{1}H NMR (300 MHz, $CDCl_3$) δ 7.91 (d, J = 8.5 Hz, ArH), 7.32 (d, J = 7.3 Hz, ArH), 6.82 (apparent t, J = 7.9 Hz, ArH), 6.5−6.7 (m, NH), 3.55−3.75 (m, NHC**H**), 2.37 (s, $ArCH_3$), 1.15 (d, J = 6.4 Hz, $CH(CH_3)_2$); MS (EI) *m*/*e* 194, 179, 132.

1-Isopropyl-6-methyl-1,2-phenylenediamine (13e). A mixture of **12e** (5.19 g, 26.7 mmol), ethanol (350 mL), and 5% Pd/C (1.3 g) was hydrogenated at room temperature for 4 h. The mixture was filtered, the solids were washed with ethanol, CH_2Cl_2, and ethanol, and the combined filtrates were concentrated to give 4.21 g (96%) of **13e** as an oil: ^{1}H NMR (300 MHz, $CDCl_3$) δ 6.80 (apparent t, J = 7.7 Hz, ArH), 6.55−6.65 (m, ArH, 2 H), 3.6−4.0 (m, NH), 3.3−3.5 (m, NHC**H**$(CH_3)_2$), 2.23 (s, $ArCH_3$), 1.13 (d, J = 6.4 Hz, $CH(CH_3)_2$).

1,2,3,4-Tetrahydro-1-isopropyl-8-methyl-2,3-dioxoquinoxaline (5e). Ethyl oxalyl chloride (3.0 mL, 27 mmol) was added to a solution of **13e** (4.21 g, 25.6 mmol), toluene (200 mL), and diisopropylethylamine (6.0 mL, 34 mmol) at −78 °C. The solution was stirred at −78 °C for 1 h and allowed to warm to room temperature over 16 h. As starting material was still present, the solution was recooled to −78 °C, and additional ethyl oxalyl chloride (1.0 mL, 9.0 mmol) and diisopropylethylamine (2.0 mL, 11 mmol) were added. After gradually warming to room temperature the solution was heated at reflux for 24 h. Upon cooling to room temperature, the residue was diluted with water (200 mL) and ether (200 mL). The solids were filtered, washed with water and ether, and dried to give 2.49 g (45%) of dione **5e** as a tan powder (mp 248−249 °C): IR (mineral oil) 1691, 1676, 1405, 778 cm^{-1}; ^{1}H NMR (300 MHz, $CDCl_3$) δ 7.0−7.15 (m, ArH, 3 H), 4.35−4.5 (m, NC**H**$(CH_3)_2$), 2.60 (s, $ArCH_3$), 1.69 (d, J = 6.7 Hz, $CH(CH_3)_2$); MS (EI) *m*/*e* 218, 176, 148.

Following this general procedure 1,2,3,4-tetrahydro-1-isopropyl-2,3-dioxoquinoxaline (**5a**), 1-*tert*-butyl-1,2,3,4-tetrahydro-2,3-dioxoquinoxaline (**5f**), 7-fluoro-1,2,3,4-tetrahydro-1-isopropyl-2,3-dioxoquinoxaline (**5c**), 7-chloro-1,2,3,4-tetrahydro-1-isopropyl-2,3-dioxoquinoxaline (**5b**), and 8-chloro-1,2,3,4-tetrahydro-1-isopropyl-2,3-dioxoquinoxaline (**5d**) were prepared.[13]

Example Procedure for the Synthesis of Benzylformamides 10. [4-(Trifluoromethyl)benzyl]formamide (10f). Ethyl formate (11.1 mL, 137 mmol) was added dropwise to

4-(trifluoromethyl)benzylamine (**9f**; 20.0 g, 114 mmol) at 0 °C. The mixture was stirred for 2 h at 0 °C and for 2 h at room temperature. Hexane was added to the solution; the resultant precipitate was filtered and dried to give 15.1 g (65%) of **10f** as a white solid (mp 70−72 °C): ^{1}H NMR (300 MHz, $CDCl_3$) δ 8.31 (s, CHO), 7.60 (d, J = 8.2 Hz, ArH, 2 H), 7.41 (d, J = 8.1 Hz, ArH, 2 H), 6.05 (br s, NH), 4.55 (d, J = 6.2 Hz, NHC**H**$_2$).

Also prepared by this method were the following compounds. [3-(Trifluoromethyl)benzyl]formamide (**10i**; 95%): ^{1}H NMR (300 MHz, $CDCl_3$) δ 8.27 (s, CHO), 7.4−7.65 (m, ArH, 4 H), 6.37 (br s, NH), 4.52 (d, J = 6.2 Hz, NHC**H**$_2$). (3-Methoxybenzyl)formamide (**10g**; 90%): ^{1}H NMR (300 MHz, $CDCl_3$) δ 8.27 (s, CHO), 7.2−7.3 (m, ArH), 6.75−6.9 (m, ArH, 3 H), 5.91 (br s, NH), 4.46 (d, J = 5.9 Hz, NHC**H**$_2$), 3.80 (s, OCH_3). (3-Fluorobenzyl)formamide (**10h**; 89%): ^{1}H NMR (300 MHz, $CDCl_3$) δ 8.29 (s, CHO), 7.2−7.45 (m, ArH), 6.85−7.2 (m, ArH, 3 H), 5.7−6.2 (br s, NH), 4.49 (d, J = 6.1 Hz, NHC**H**$_2$). (4-Chlorobenzyl)formamide (**10d**; 83%): ^{1}H NMR (300 MHz, $CDCl_3$) δ 8.27 (s, CHO), 7.15−7.4 (m, ArH, 4 H), 5.96 (br s, NH), 4.45 (d, J = 6.1 Hz, $ArCH_2$). (4-Fluorobenzyl)formamide (**10e**; 88%): ^{1}H NMR (300 MHz, $CDCl_3$) 8.21 (s, CHO), 7.15−7.3 (m, ArH, 2 H), 6.95−7.05 (m, ArH, 2 H), 6.37 (br s, NH), 4.41 (d, J = 6.0 Hz, $ArCH_2$).

Example Procedure for the Synthesis of Benzyl Isocyanides 7. 4-(Trifluoromethyl)benzyl Isocyanide (7f). Phosphorus oxychloride (6.9 mL, 74 mmol) was added dropwise to a solution of formamide **10f** (15.1 g, 74.3 mmol), triethylamine (31.0 mL, 222 mmol), and CH_2Cl_2 (200 mL) at 0 °C. The solution was stirred at 0 °C for 1 h, and aqueous sodium carbonate (7.85 g in 100 mL of H_2O, 74.1 mmol) was added. Stirring was continued for 1 h. Aqueous workup (CH_2Cl_2, $MgSO_4$) and purification by flash chromatography (5 → 20% ethyl acetate/hexane) provided 10.4 g (76%) of **7f** as an off-white solid: ^{1}H NMR (300 MHz, $CDCl_3$) δ 7.68 (d, J = 8.2 Hz, ArH, 2 H), 7.49 (d, J = 8.1 Hz, ArH, 2 H), 4.73 (s, NCH_2).

Also prepared by this procedure were the following compounds. 3-(Trifluoromethyl)benzyl isocyanide (**7i**; 86%): ^{1}H NMR (300 MHz, $CDCl_3$) δ 7.5−7.7 (m, ArH, 4 H), 4.73 (s, NCH_2). 3-Methoxybenzyl isocyanide (**7g**; 86%): ^{1}H NMR (300 MHz, $CDCl_3$) δ 7.25−7.35 (m, ArH), 6.85−6.95 (m, ArH, 3 H), 4.61 (s, NCH_2), 3.82 (s, OCH_3). 3-Fluorobenzyl isocyanide (**7h**; 80%): ^{1}H NMR (300 MHz, $CDCl_3$) δ 7.3−7.45 (m, ArH), 7.0−7.2 (m, ArH, 3 H), 4.66 (s, ArC**H**$_2$N). 4-Chlorobenzyl isocyanide (**7d**; 72%): ^{1}H NMR (300 MHz, $CDCl_3$) δ 7.35−7.4 (m, ArH, 2 H), 7.25−7.35 (m, ArH, 2 H), 4.61 (s, $ArCH_2$). 4-Fluorobenzyl isocyanide (**7e**; 84%): ^{1}H NMR (300 MHz, $CDCl_3$) δ 7.3−7.4 (m, ArH, 2 H), 7.0−7.15 (m, ArH, 2 H), 4.62 (s, CH_2).

Example Procedure for the Preparation of Isocyanides 7 Directly from 9. 4-Methylbenzyl Isocyanide (7c). Aqueous 50% NaOH (12 mL) was added to a mixture of 4-methylbenzylamine (**9c**; 5.00 g, 41.3 mmol), benzyltriethylammonium chloride (114 mg, 0.502 mmol), chloroform (4.93 g, 41.3 mmol), and CH_2Cl_2 (12 mL). The mixture was heated at 50 °C for 3.5 h. After cooling to room temperature, aqueous workup (CH_2Cl_2, brine, Na_2SO_4) and purification by flash chromatography (30% ethyl acetate/hexane) provided 2.63 g (49%) of **7c** as a yellow oil: ^{1}H NMR (300 MHz, $CDCl_3$) δ 7.1−7.3 (m, ArH, 4 H), 4.59 (s, $ArCH_2$), 2.37 (s, $ArCH_3$).

Also prepared by this procedure were the following compounds. 2-Methoxybenzyl isocyanide (**7j**; 43%): ^{1}H NMR (300 MHz, $CDCl_3$) 7.35 (d, J = 7.4 Hz, ArH), 7.2−7.35 (m, ArH), 6.94 (dd, J = 8.2, 7.6 Hz, ArH), 6.82 (d, J = 8.3 Hz, ArH), 4.56 (s, $ArCH_2$), 3.78 (s, OCH_3). 4-Methoxybenzyl isocyanide (**7b**; 46%): ^{1}H NMR (300 MHz, $CDCl_3$) δ 7.2−7.3 (m, ArH, 2 H), 6.85−6.95 (m, ArH, 2 H), 4.56 (narrow m, $ArCH_2$), 3.81 (s, OCH_3).

Example Procedure for Cyclization of 5 with Isocyanide 7. Method A. 5-(1-Methylethyl)-3-phenylimidazo-[1,5-*a*]quinoxalin-4(5*H*)-one (23). Quinoxaline **5a** (1.00 g, 4.90 mmol) was added to a mixture of hexane-washed sodium hydride (254 mg, 6.35 mmol, 60% mineral oil dispersion) and DMF (10.8 mL). The solution was stirred for 30 min at room temperature and cooled to −10 °C. Diethyl chlorophosphate (0.92 mL, 6.4 mmol) was added, and the solution was allowed to warm to room temperature. After 1 h the solution was cooled to 0 °C. A mixture of potassium *tert*-butoxide (711 mg, 6.34 mmol) and DMF (1.5 mL) was cooled to −42 °C. Isocyanide **7a** (0.77 mL, 6.3 mmol) was added and the mixture allowed to warm to 0 °C. This mixture was transferred to the solution of the quinoxaline which was then allowed to warm to room temperature. After 1 h the reaction was quenched with 1.0 mL of acetic acid, and the mixture was concentrated. The residue was triturated with ethyl acetate to provide 580 mg of **23** as a white powder. The filtrate was concentrated and purified by flash chromatography (20:1 CH_2Cl_2:acetone) to provide an additional 189 mg (0.769 g total, 52%) of the desired product. An analytical sample was prepared by recrystallization from CH_2Cl_2/hexane (mp 207−208 °C): IR (mineral oil) 3089, 1662, 1656, 1515, 1501, 1478, 1304, 1298, 1221, 745, 692 cm^{-1}; ^{1}H NMR (300 MHz, $CDCl_3$) δ 8.46 (s, ArH), 8.17 (dd, J = 8.5, 1.5 Hz, ArH, 2 H), 7.80 (d, J = 8.1 Hz, ArH), 7.54 (d, J = 8.5 Hz, ArH), 7.15−7.5 (m, ArH, 5 H), 5.2−5.6 (br s, C**H**$(CH_3)_2$), 1.65 (d, J = 7.0 Hz, CH(C**H**$_3)_2$); MS (EI) m/e 303, 261. Anal. ($C_{19}H_{17}N_3O$) C, H, N.

Example Procedure for Cyclization of 5 with Isocyanide 7. Method B. 3-(3-Fluorophenyl)-5-(1-methylethyl)-imidazo[1,5-*a*]quinoxalin-4(5*H*)-one (30). Potassium *tert*-butoxide (5.20 mL, 5.20 mmol, 1.0 M in THF) was added to a mixture of **5a** (1.00 g, 4.90 mmol) and THF (20.0 mL) at −20 °C. The mixture was allowed to warm to 0 °C over 45 min and was cooled to −40 °C. Diethyl chlorophosphate (0.75 mL, 5.2 mmol) was added, and the mixture was allowed to warm to room temperature over 30 min. The resultant solution was cooled to −78 °C, and a solution of isocyanide **7h** (723 mg, 5.35 mmol) and THF (1.0 mL) was added. Potassium *tert*-butoxide (5.20 mL, 5.20 mmol) was then added dropwise over several minutes. The solution was stirred at −78 °C for 30 min and allowed to warm to room temperature over 2.5 h. After stirring at room temperature for 2 h, water was added. The solids were collected, washed with water (3 × 30 mL) and ether (3 × 30 mL), and dried *in vacuo* to give 1.04 g of **30**. Recrystallization from hot EtOAc/MeOH/hexane gave 866 mg of **30** as a white wool-like material (mp 215−217 °C). Aqueous workup (ethyl acetate, $MgSO_4$) of the combined filtrates, purification by flash chromatography (3:1 hexane:ethyl acetate), and recrystallization as above provided an additional 306 mg (1.17 g total, 74%) of product: IR (mineral oil) 3092, 1663, 1656, 1613, 1515, 1501, 1323, 1301, 1223, 750 cm^{-1}; ^{1}H NMR (300 MHz, $CDCl_3$) δ 8.47 (s, ArH), 7.95−8.1 (m, ArH, 2 H), 7.83 (d, J = 8.4 Hz, ArH), 7.57 (d, J = 8.4 Hz, ArH), 7.35−7.5 (m, ArH, 2 H), 7.2−7.35 (m, ArH), 7.0−7.15 (m, ArH), 5.2−5.5 (m, C**H**$(CH_3)_2$), 1.67 (d, J = 7.1 Hz, CH(C**H**$_3)_2$); MS (EI) m/e 321, 279. Anal. ($C_{19}H_{16}N_3OF\cdot(H_2O)_{1/8}$) C, H, N.

5-*tert*-Butyl-3-(4-fluorophenyl)imidazo[1,5-*a*]quinoxalin-4(5*H*)-one (8a, R^1 = tBu). Following procedure B, but using 5.00 g (22.9 mmol) of **5f** and purification by flash chromatography (1:2 → 1:1 ethyl acetate:hexane), gave 4.53 g (59%) of the desired product as a light yellow powder (mp 135−137 °C): IR (mineral oil) 1668, 1498, 1299, 751 cm^{-1}; ^{1}H NMR (300 MHz, $CDCl_3$) δ 8.31 (s, ArH), 8.22 (dd, J = 8.9, 5.6 Hz, ArH, 2 H), 7.63 (d, J = 7.9 Hz, ArH), 7.55 (d, J = 7.1 Hz, ArH), 7.05−7.35 (m, ArH, 4 H), 1.76 (s, tBu); MS (EI) m/e 335, 279.

5-*tert*-Butyl-3-(4-fluorophenyl)-4,5-dihydroimidazo[1,5-*a*]quinoxaline (18a, R^1 = tBu). A solution of **8a** (R^1 = tBu; 1.32 g, 3.94 mmol), THF (50.0 mL), and borane−methyl sulfide complex (2.6 mL, 26 mmol, 10.0 M) was heated at reflux for 24 h. After cooling to room temperature, excess hydride was quenched with 10% HCl. Basic workup (ethyl acetate, $NaHCO_3$, $MgSO_4$) and purification by flash chromatography (1.5:1 hexane:ethyl acetate) gave 730 mg (58%) of the quinoxaline as a white solid (mp 129−130 °C): IR (mineral oil) 1504, 1215, 1203, 842, 751 cm^{-1}; ^{1}H NMR (300 MHz, $CDCl_3$) δ 8.06 (s, ArH), 7.6−7.75 (m, ArH, 2 H), 7.45−7.55 (m, ArH), 7.1−7.4 (m, ArH, 5 H), 4.46 (s, NCH_2), 1.00 (s, tBuN); MS (EI) m/e 321, 306, 264.

3-(4-Fluorophenyl)-4,5-dihydroimidazo[1,5-*a*]quinoxaline (19a). A solution of amine **18a** (R^1 = tBu; 728 mg, 2.27 mmol), CH_2Cl_2 (20.0 mL), and trifluoroacetic acid (20.0 mL) was stirred at room temperature for 72 h. Concentration and basic workup (CH_2Cl_2, $NaHCO_3$, $MgSO_4$) gave 574 mg (95%) of the desired product as a white foam, homogeneous by TLC analysis: IR (mineral oil) 3381, 1511, 1492, 1290, 1231, 838,

741 cm^{-1}; ^1H NMR (300 MHz, $CDCl_3$) δ 8.04 (s, ArH), 7.58 (dd, J = 8.8, 5.4 Hz, ArH, 2 H), 7.42 (d, J = 6.8 Hz, ArH), 7.0−7.2 (m, ArH, 3 H), 6.8−6.95 (m, ArH, 2 H), 4.66 (d, J = 1.7 Hz, NHC**H**$_2$), 4.07 (br s, NH); MS (EI) *m/e* 265, 264, 237, 144, 118.

Also prepared by this procedure was 4,5-dihydro-3-(4-methoxyphenyl)imidazo[1,5-*a*]quinoxaline (**19b**) (mp 177−180 °C): IR (mineral oil) 3379, 1511, 1497, 1297, 1249, 1240, 739 cm^{-1}; ^1H NMR (300 MHz, $CDCl_3$) δ 8.04 (s, ArH), 7.5−7.6 (m, ArH, 2 H), 7.42 (d, J = 8.0 Hz, ArH), 7.07 (apparent t, J = 7.7 Hz, ArH), 6.9−7.05 (m, ArH, 2 H), 6.75−6.9 (m, ArH, 2 H), 4.66 (d, J = 1.6 Hz, NCH_2), 4.08 (s, NH), 3.85 (s, OCH_3); MS (EI) *m/e* 277, 276, 144.

5-*tert*-Butyl-3-*p*-tolylimidazo[1,5-*a*]quinoxalin-4(5*H*)-one (8c, R^1 = tBu). Following procedure B using 5.00 g (22.9 mmol) of **5f** and purification by flash chromatography (20% ethyl acetate/hexane) provided 3.32 g (44%) of the product as a light yellow solid (mp 160−165 °C): IR (mineral oil) 1668, 1502, 1295, 1186, 748 cm^{-1}; ^1H NMR (300 MHz, $CDCl_3$) δ 8.31 (s, ArH), 8.10 (d, J = 8.2 Hz, ArH, 2 H), 7.62 (d, J = 7.9 Hz, ArH), 7.53 (d, J = 8.3 Hz, ArH), 7.15−7.35 (m, ArH, 4 H), 2.40 (s, $ArCH_3$), 1.75 (s, $C(CH_3)_3$); MS (EI) *m/e* 331, 275.

3-*p*-Tolylimidazo[1,5-*a*]quinoxalin-4(5*H*)-one (20c). Trifluoroacetic acid (59 mL) was added to a solution of amide **8c** (R^1 = tBu; 2.95 g, 8.90 mmol) in CH_2Cl_2 (59 mL) at 0 °C. The mixture was allowed to warm to room temperature over 2 h and concentrated. The solids were filtered, washed with water, and dried to give 2.30 g (94%) of the deprotected amide as a white solid (mp >300 °C): IR (mineral oil) 1686, 1654, 1494, 1376, 823 cm^{-1}; ^1H NMR (300 MHz, DMSO-d_6) δ 11.39 (s, NH), 9.16 (s, ArH), 8.20 (apparent d, J = 8.1 Hz, ArH, 3 H), 7.2−7.45 (m, ArH, 5 H), 2.36 (s, CH_3); MS (EI) *m/e* 275, 247, 219.

4,5-Dihydro-3-*p*-tolylimidazo[1,5-*a*]quinoxaline (19c). Aluminum hydride[37] (50 mL, 32 mmol, 0.63 M in THF) was added to **20c** (1.60 g, 5.81 mmol) and the mixture stirred at room temperature for 2 days and heated at reflux for 16 h. After cooling to room temperature, excess aluminum hydride was decomposed by adding methanol (20 mL) and 6 N NaOH (50 mL). Aqueous workup (CH_2Cl_2, $MgSO_4$) and trituration in 75% ether/hexane gave 1.15 g (75%) of a beige powder containing product and starting material[38] (10:1) which was carried on crude. Spectral data for a pure sample[39] of **19c** (mp 189−194 °C): IR (mineral oil) 1522, 1507, 1288, 959, 742, 735 cm^{-1}; ^1H NMR (300 MHz, DMSO-d_6) δ 8.43 (s, ArH), 7.66 (d, J = 8.4 Hz, ArH), 7.50 (d, J = 8.1 Hz, ArH, 2 H), 7.23 (d, J = 8.0 Hz, ArH, 2 H), 6.95−7.1 (m, ArH), 6.87 (d, J = 7.7 Hz, ArH), 6.74 (apparent t, J = 7.9 Hz, ArH), 6.31 (s, NH), 4.57 (s, NCH_2), 2.33 (s, $ArCH_3$); MS (EI) *m/e* 261, 260, 231, 219, 144, 116.

Also prepared by this procedure was 4,5-dihydro-3-phenylimidazo[1,5-*a*]quinoxaline (**19d**) (mp 187−189 °C): IR (mineral oil) 3382, 1616, 1523, 766, 736, 692 cm^{-1}; ^1H NMR (300 MHz, $CDCl_3$) δ 8.12 (s, ArH), 7.62 (dd, J = 8.5, 1.3 Hz, ArH, 2 H), 7.35−7.5 (m, ArH, 3 H), 7.25−7.35 (m, ArH), 7.0−7.15 (m, ArH), 6.75−6.95 (m, ArH, 2 H), 4.68 (s, NCH_2); MS (EI) *m/e* 247, 246, 219, 144, 109.

3-Chloro-*N*-(3,4-dimethoxybenzyl)-6-nitroaniline (12g). A mixture of veratrylamine (12.2 g, 73.0 mmol), 2,4-dichloronitrobenzene (**11**, R^6 = H, R^7 = Y = Cl; 12.9 g, 67.2 mmol), and diisopropylethylamine (27.9 mL, 160 mmol) was stirred at room temperature for 6 days and at 75 °C for 7 days. Additional veratrylamine (10.0 g, 59.8 mmol) and diisopropylethylamine (10.0 mL, 57.3 mmol) were added at 8 and 2 days, respectively. After cooling to room temperature, aqueous workup (ethyl acetate, 10% HCl, $NaHCO_3$, brine washes, $MgSO_4$), and purification by flash chromatography (5:1 hexane:ethyl acetate) gave 16.4 g (76%) of **12g** as an orange solid (mp 106−107 °C): IR (mineral oil) 1565, 1524, 1491, 1309, 1259, 1211 cm^{-1}; ^1H NMR (300 MHz, $CDCl_3$) δ 8.3−8.4 (m, NH), 8.15 (d, J = 9.1 Hz, ArH), 6.8−6.95 (m, ArH, 4 H), 6.64 (dd, J = 9.2, 2.2 Hz, ArH), 4.44 (d, J = 5.4 Hz, NHC**H**$_2$), 3.90 (s, OCH_3), 3.89 (s, OCH_3); MS (EI) *m/e* 322, 304, 165, 151.

4-Chloro-2-[(3,4-dimethoxybenzyl)amino]aniline (13g). A mixture of **12g** (16.4 g, 50.8 mmol), ethanol (900 mL), and platinum on sulfide carbon (1.5 g) was hydrogenated at 30 psi for 16 h. The mixture was filtered, the residual solids were washed with MeOH and CH_2Cl_2, and the filtrate was concentrated to provide 14.3 g (96%) of **13g** as a dark solid which was carried on crude: ^1H NMR (300 MHz, $CDCl_3$) δ 6.8−7.0 (m, ArH, 3 H), 6.65 (narrow m, ArH, 3 H), 4.21 (s, NCH_2), 3.89 (s, OCH_3, 6 H).

7-Chloro-1,2,3,4-tetrahydro-1-(3,4-dimethoxybenzyl)-2,3-dioxoquinoxaline (5g). Ethyl oxalyl chloride (1.70 mL, 15.2 mmol) was added to a solution of **13g** (4.21 g, 14.4 mmol), toluene (105 mL), THF (100 mL), and diisopropylethylamine (3.26 mL, 18.7 mmol) at −78 °C. The mixture was stirred at −78 °C for 1 h and allowed to warm to room temperature overnight. The reaction mixture was heated at reflux for 24 h and allowed to cool to room temperature. The mixture was filtered; the solids were washed extensively with water and ether and dried to provide 4.40 g (88%) of **5g** as a gray powder (mp 277−280 °C): IR (mineral oil) 1699, 1682, 1522, 1470, 1462, 1444, 1265, 1250, 1140, 1020, 845 cm^{-1}; ^1H NMR (300 MHz, DMSO-d_6) δ 12.17 (s, NH), 7.27 (s, ArH, 2 H), 7.1−7.25 (m, ArH, 2 H), 7.02 (s, ArH), 6.87 (d, J = 8.4 Hz, ArH), 6.79 (d, J = 7.7 Hz, ArH), 5.28 (s, NCH_2), 3.72 (s, OCH_3), 3.70 (s, OCH_3); MS (EI) *m/e* 346, 151.

7-Chloro-3-(4-fluorophenyl)-5-(3,4-dimethoxybenzyl)-imidazo[1,5-*a*]quinoxalin-4(5*H*)-one (8e). Following procedure B, but starting with **5g** (9.35 g, 27.0 mmol), gave 7.86 g (63%) of the quinoxaline as a gray powder (mp 237−239 °C): IR (mineral oil) 1656, 1521, 1501, 1287, 1239, 1135 cm^{-1}; ^1H NMR (300 MHz, $CDCl_3$) δ 8.53 (s, ArH), 8.27 (dd, J = 9.2, 5.4 Hz, ArH, 2 H), 7.75 (d, J = 8.7 Hz, ArH), 7.31 (narrow m, ArH), 7.1−7.3 (m, ArH, 3 H), 6.8−6.9 (m, 3 H), 5.38 (s, NCH_2), 3.86 (s, OCH_3), 3.85 (s, OCH_3); MS (EI) *m/e* 463, 151, 107.

7-Chloro-3-(4-fluorophenyl)-4,5-dihydroimidazo[1,5-*a*]-quinoxaline (19e). A mixture of **8e** (2.00 g, 4.31 mmol), lithium aluminum hydride (720 mg, 19.0 mmol), and THF (75 mL) was stirred at room temperature for 4 days. Water (0.7 mL), 10% KOH (1.0 mL), and water (2.0 mL) were added successively. The mixture was stirred for 1 h and filtered. The solids were washed with EtOAc and CH_2Cl_2 several times. The combined filtrates were dried ($MgSO_4$), filtered, and concentrated to give 1.84 g of a mixture of crude **18e** and starting material.

The residue was combined with CH_2Cl_2 (30 mL) and anisole (1.1 mL, 10 mmol) and the solution cooled to 0 °C. Trifluoroacetic acid (30 mL) was added, and the solution was stirred for 1 h at 0 °C and for 16 h at room temperature. Concentration and basic workup (CH_2Cl_2, $NaHCO_3$, $MgSO_4$) gave **19e**, contaminated by trace amounts of the corresponding imine. Sodium borohydride (1.25 g, 33.0 mmol) was added to a solution of the crude material and ethanol (100 mL). The solution was stirred at room temperature for 3 h and concentrated. Aqueous workup (CH_2Cl_2, $MgSO_4$) and purification by flash chromatography (1:1 hexane:ethyl acetate; 1% CH_2Cl_2) gave 623 mg (48% overall) of the product as a white solid (mp 186−189 °C): IR (mineral oil) 1609, 1516, 1506, 1290, 1263, 1237, 1158, 840, 832 cm^{-1}; ^1H NMR (300 MHz, $CDCl_3$) 8.02 (s, ArH), 7.5−7.7 (m, ArH, 2 H), 7.35 (d, J = 7.7 Hz, ArH), 7.12 (apparent t, J = 9.2 Hz, ArH, 2 H), 6.8−7.0 (m, ArH, 2 H), 4.67 (s, NCH_2), 4.17 (s, NH); MS (EI) *m/e* 299, 298, 178, 151.

Also prepared by this procedure were the following compounds. 6-Chloro-3-(4-fluorophenyl)-4,5-dihydroimidazo[1,5-*a*]quinoxaline (**19f**) (mp 146−149 °C): IR (mineral oil) 1505, 1222, 837, 757 cm^{-1}; ^1H NMR (300 MHz, $CDCl_3$) δ 8.04 (s, ArH), 7.58 (dd, J = 8.8, 5.4 Hz, ArH, 2 H), 7.35 (d, J = 8.1 Hz, ArH), 7.05−7.25 (m, ArH, 3 H), 6.80 (apparent t, J = 8.1 Hz, ArH), 4.74 (d, J = 1.7 Hz, $HNCH_2$), 4.68 (s, NH); MS (EI) *m/e* 299, 298, 178, 118. 7-Fluoro-3-(4-fluorophenyl)-4,5-dihydroimidazo[1,5-*a*]quinoxaline (**19g**) (mp 175 °C): IR (mineral oil) 1526, 1507, 1272, 1158, 836 cm^{-1}; ^1H NMR (300 MHz, DMSO-d_6) δ 9.06 (s, HC=N), 7.7−7.85 (m, ArH), 7.6−7.75 (m, ArH, 2 H), 7.34 (apparent t, J = 12.0 Hz, ArH, 2 H), 6.55−6.8 (m, ArH, 2 H), 4.64 (s, NCH_2); MS (EI) *m/e* 283, 282, 255, 162, 127.

Example Procedure for Carbamoyl Chlorides 22. 6-Chloro-5-(chlorocarbonyl)-3-(4-fluorophenyl)-4,5-dihydroimidazo[1,5-*a*]quinoxaline (22f). Phosgene (9.3 mL, 18 mmol, 1.93 M in toluene) was added dropwise to a solution of

19f (1.80 g, 6.01 mmol), diisopropylethylamine (3.14 mL, 18.0 mmol), THF (17 mL), and CH_2CH_2 (17 mL) at room temperature. The mixture was stirred at room temperature overnight. Aqueous workup (ethyl acetate, $MgSO_4$) gave 2.16 g (99%) of **22f** as a yellow oil which was carried on crude.

Example Procedure for the Reaction of Carbamoyl Chlorides 22 with Amines. Method C. 6-Chloro-5-[[1-(3,5-dimethylpiperazino)]carbonyl]-3-(4-fluorophenyl)-4,5-dihydroimidazo[1,5-*a*]quinoxaline (69). To a solution of **22f** (1.44 g, 3.98 mmol) and diisopropylethylamine (0.92 mL, 5.3 mmoL) in THF (20 mL) at 0 °C was added *cis*-2,6-dimethylpiperazine (543 mg, 4.76 mmol). The mixture was allowed to warm slowly and stirred at room temperature for 4 days. Aqueous workup (CH_2Cl_2, $MgSO_4$) and purification by flash chromatography (4% methanol/CH_2Cl_2) provided 1.12 g (64%) of **69** as a yellow solid. An analytical sample was prepared by recrystallization from ethyl acetate/hexane to give a light yellow solid (mp 203−205 °C): IR (mineral oil) 1659, 1507, 1494, 1410, 1258, 1225, 831, 780 cm^{-1}; ^1H NMR (300 MHz, $CDCl_3$) δ 8.08 (s, ArH), 7.55−7.65 (m, ArH, 2 H), 7.50 (d, J = 7.9 Hz, ArH), 7.35 (d, J = 7.0 Hz, ArH), 7.2−7.3 (m, ArH), 7.16 (apparent t, J = 8.7 Hz, ArH, 2 H), 4.85 (s, $ArNCH_2$), 3.73 (d, J = 13.8 Hz, 2 H), 2.8−3.0 (m, 2 H), 2.4−2.6 (m, 2 H), 1.04 (d, J = 7.6 Hz, $CHCH_3$, 6 H); MS (EI) *m/e* 439, 404, 382, 361, 321, 298, 141. Anal. ($C_{23}H_{23}N_5OClF$) C, H, N, Cl.

Example Procedure for the Reaction of Carbamoyl Chlorides 22 with Alcohols. Method D. Methyl 3-(4-Fluorophenyl)-4,5-dihydroimidazo[1,5-*a*]quinoxaline-5-carboxylate (59). Sodium methoxide (180 mg of sodium in 6.0 mL of MeOH, 7.8 mmol) was added to a mixture of carbamoyl chloride **22a** (2.30 mmol) and MeOH (10.0 mL) at 0 °C. The mixture was stirred for 1 h at 0 °C and for 16 h at room temperature. Acetic acid (0.50 mL) was added and the mixture concentrated. Aqueous workup (CH_2Cl_2, $MgSO_4$) and purification by flash chromatography (1:1 hexane:ethyl acetate) gave 447 mg of an oil which was crystallized from hexane/ether to provide 258 mg (35%) of **59** as a yellow powder (mp 156−160 °C): IR (mineral oil) 1709, 1505, 1435, 1368, 1223 cm^{-1}; ^1H NMR (300 MHz, $CDCl_3$) δ 8.07 (s, ArH), 7.6−7.8 (m, ArH), 7.65 (dd, J = 8.8, 5.4 Hz, ArH, 2 H), 7.5−7.6 (m, ArH), 7.25−7.35 (m, ArH, 2 H), 7.16 (apparent t, J = 8.8 Hz, ArH, 2 H), 5.11 (s, NCH_2), 3.81 (s, OCH_3); MS (EI) *m/e* 323, 308, 264, 236. Anal. ($C_{18}H_{14}N_3O_2F$) C, H, N.

Synthesis of Ureas 16 Directly from Amines 19. Method E. 4,5-Dihydro-5-(pyrrolidinocarbonyl)-3-*p*-tolylimidazo[1,5-*a*]quinoxaline (46). A mixture of **19c** (450 mg, 1.72 mmol), diisopropylethylamine (0.35 mL, 2.0 mmol), and CH_2Cl_2 (25 mL) was cooled to 0 °C. Triphosgene (276 mg, 0.930 mmol) was added and the solution allowed to warm to room temperature. After stirring at room temperature for 1 h, the solution was cooled to 0 °C and pyrrolidine (0.55 mL, 6.6 mmol) was added. The solution was allowed to warm and stirred at room temperature for 2 h. Aqueous workup (CH_2Cl_2, $MgSO_4$) and purification by flash chromatography (20 → 50% ethyl acetate/hexane) provided, after drying *in vacuo*, 498 mg (81%) of **46** as a white solid (mp 238.5−239.5 °C): IR (mineral oil) 1636, 1506, 1413, 752 cm^{-1}; ^1H NMR (300 MHz, $CDCl_3$) δ 8.07 (s, ArH), 7.45−7.65 (m, ArH, 3 H), 7.1−7.3 (m, ArH, 5 H), 4.91 (s, $ArNCH_2$), 3.25 (br s, CH_2NCH_2), 2.38 (s, $ArCH_3$), 1.7−1.85 (m, $NCH_2CH_2CH_2$); MS (EI) *m/e* 358, 260, 98. Anal. ($C_{22}H_{22}N_4O$) C, H, N.

General Procedure for the Acylation of 19 To Provide 21. Method F. 3-(4-Fluorophenyl)-5-(2-fluorobenzoyl)-4,5-dihydroimidazo[1,5-*a*]quinoxaline (63). 2-Fluorobenzoyl chloride (0.29 mL, 2.4 mmol) was added to a solution of amine **19a** (600 mg, 2.26 mmol), diisopropylethylamine (0.47 mL, 2.7 mmol), and THF (20 mL) at 0 °C. The solution was stirred at 0 °C for 1.5 h and allowed to warm to room temperature. After stirring for 16 h, aqueous workup (ethyl acetate, $MgSO_4$), purification by flash chromatography (1:1 hexane:ethyl acetate), and crystallization from ethyl acetate/hexane gave 680 mg (78%) of **63** as light yellow crystals (mp 185−189 °C): IR (mineral oil) 1656, 1507, 1284, 1219, 751 cm^{-1}; ^1H NMR (300 MHz, $CDCl_3$) δ 8.15 (s, ArH), 6.6−7.75 (m, ArH, 12 H), 5.0−5.5 (m, NCH_2); MS (EI) *m/e* 387, 123. Anal. ($C_{23}H_{15}N_3OF_2$) C, H, N.

General Reductive Amination Procedure for 3,4,5-Trimethylpiperazines. Method G. 6-Chloro-3-(4-fluorophenyl)-4,5-dihydro-5-[[1-(3,4,5-trimethylpiperazino]-carbonyl]imidazo[1,5-*a*]quinoxaline (70). Sodium cyanoborohydride (236 mg, 3.76 mmol) was added to a solution of **69** (550 mg, 1.25 mmol) and formaldehyde (37%, 1.9 mL, 25 mmol) in methanol (8 mL) at room temperature. The mixture was stirred overnight at room temperature. Aqueous workup (ethyl acetate, $MgSO_4$) and recrystallization from ethyl acetate/hexane provided 460 mg (81%) of the desired compound as a yellow solid (mp 213−214 °C): IR (mineral oil) 1657, 1500, 1448, 1416, 1232, 1222, 836 cm^{-1}; ^1H NMR (300 MHz, $CDCl_3$) δ 8.08 (s, ArH), 7.58 (dd, J = 8.8, 5.4 Hz, ArH, 2 H), 7.50 (dd, J = 7.9, 1.4 Hz, ArH), 7.35 (dd, J = 8.2, 1.3 Hz, ArH), 7.2−7.3 (m, ArH, 1 H), 7.16 (apparent t, J = 8.7 Hz, ArH, 2 H), 4.85 (s, $ArNCH_2$), 3.66 (d, J = 15.5 Hz, 2 H), 2.77 (apparent t, J = 11.5 Hz, 2 H), 2.26 (s, NCH_3), 2.15−2.35 (m, 2 H), 1.07 (d, J = 6.1 Hz, $CHCH_3$, 6 H); MS (EI) *m/e* 453, 418, 382, 361, 297, 278, 155, 141, 113, 98, 84, 72. Anal. ($C_{24}H_{25}N_5OClF$) C, H, N, Cl.

$GABA_A$ Receptor Expression and Membrane Preparation. DNA manipulations and general baculovirus methods (Sf-9 cell cultivation, infection, and isolation; purification of recombinant viruses) were performed as described elsewhere.[24] The Sf-9 cells were infected at a multiplicity of infection of 3 PFU of viruses: AcNPV-α_1, -α_3 or -α_6, AcNPV-β_2, and AcNPV-γ_2. Infected cells were used for electrophysiological measurements at 48 h postinfection or for membrane preparations at 60 h postinfection. The stable cell lines expressing α_1, α_3, or α_6, β_2, and γ_2 subunits of $GABA_A$ were derived by transfection of plasmids containing cDNA and a plasmid encoding G418 resistance into human kidney cells (A293 cells) as described elsewhere.[25] After 2 weeks of selection in 1 mg/mL G418, cells positive for all three $GABA_A$ receptor mRNAs by Northern blotting were used for electrophysiology to measure GABA-induced Cl^- currents.

For equilibrium binding measurements, Sf-9 cells infected with baculovirus-carrying cDNAs for α_1, α_3, or α_6, β_2, and γ_2 subunits were harvested in 2 L batches at 60 h postinfection. The membranes were prepared following the procedure described previously.[24] Briefly, the membranes were prepared in normal saline after homogenization with a Polytron PT 3000 homogenizer (Brinkman) for 4 min. Unbroken cells and large nuclei aggregates were removed by centrifugation at 1000*g* for 10 min. Then the membranes were recovered with the second centrifugation of the supernatant at 40000*g* for 50 min. The membranes were resuspended to a final concentration of 5 mg/mL in a solution containing 300 mM sucrose, 5 mM Tris/HCl, pH 7.5, and glycerol to a final concentration of 20% and stored at −80 °C. Equilibrium binding of [^{3}H]flunitrazepam or [^{3}H]Ro-4513 to the cloned $GABA_A$ receptors was measured in a 500 mL volume of normal saline containing 6 nM [^{3}H]-flunitrazepam or [^{3}H]Ro-4513, varying concentrations of test ligands, and 50 mg of membrane protein. The mixture was incubated for 60 min at 4 °C, filtered over a Whatman glass fiber filter, and washed four times with cold normal saline. The filter was then counted for radioactivity in the presence of a scintillation cocktail (Insta Gel).

$GABA_A$ Receptor Binding. The *in vitro* binding affinity of the imidazo[1,5-*a*]quinoxalines for $GABA_A$ was determined as previously described with minor modification.[15] Freshly prepared rat cerebellar membranes were suspended in 300 mM sucrose and 10 nM Hepes/Tris, pH 7.4. Typically, the reaction medium contained 6 mM [^{3}H]flunitrazepam, 50 mg of membrane protein, test drugs at various concentrations or vehicle in 200 mL, 118 mM NaCl, 10 mM Hepes/Tris, pH 7.4, and 1 mM $MgCl_2$. The mixtures were incubated for 60 min at 4 °C. The amount of binding was determined with rapid filtration techniques using Whatman GF/B filters.

[^{35}S]-*tert*-Butyl Bicyclophosphorothionate ([^{35}S]TBPS) Binding. Binding of [^{35}S]TBPS in the rat brain membranes was measured in the medium containing 2 nM [^{35}S]TBPS, unless specified otherwise, 50 mg of membrane proteins, 1 M NaCl, and 10 mM Tris/HCl, pH 7.4, in a total volume of 500

mL. Drugs were added in concentrated methanolic solutions, and the level of methanol did not exceed 0.2% and was maintained constant in all tubes. The mixtures were incubated for 120 min at 24 °C. The reaction mixtures were filtered over a Whatman GF/B filter under vacuum. The filters were washed three times with 4 mL of the reaction buffer without radioisotope and counted for radioactivity. Nonspecific binding was estimated in the presence of 2 mM unlabeled TBPS and subtracted to compute specific binding.[16]

Electrophysiology. The whole cell configuration of the patch clamp technique was used to record the GABA-mediated Cl^- currents in the A293 cells expressing the $\alpha_1\beta_2\gamma_2$ subtype, as described earlier.[18] Briefly, patch pipets made of borosilicate glass tubes were fire-polished and showed a tip resistance of 0.5 −2 MΩ when filled with a solution containing (mM) 140 CsCl, 11 EGTA, 4 $MgCl_2$, 2 ATP, and 10 Hepes, pH 7.3. The cell-bathing external solution contained (mM) 135 NaCl, 5 KCl, 1 $MgCl_2$, 1.8 $CaCl_2$, and 5 Hepes, pH 7.2 (normal saline). GABA at the concentration of 5 mM in the external solution with or without indicated drugs was applied through a U-tube placed within 100 mm of the cells for 10 s, unless indicated otherwise. The current was recorded with an Axopatch 1D amplifier and a CV-4 headstage (Axon Instrument Co.). A Bh-1 bath headstage was used to compensate for changes in bath potentials. The currents were recorded with a Gould Recorder 220. GABA currents were measured at the holding potential of −60 mV at room temperature (21−24 °C).

Metrazole Antagonism. Compounds were tested for their ability to antagonize metrazole-induced convulsions in mice after ip injection as described elsewhere.[19] Briefly, male CF-1 mice were injected with metrazole (85 mg/kg, sc), and convulsive seizure was elicited 15 min later with an auditory stimulation (5 dB for 10 s). Drugs tested for metrazole antagonism were injected ip 30 min before the metrazole challenge, 4 mice/dose at a 0.3 log dose interval. ED_{50}'s for protection against tonic seizure were calculated by the method of Spearman-Karber (Finney, D. J. *Statistical Methods in Biological Assay*).

Ethanol Potentiation. Male CF-1 Charles River mice were injected orally with 7.5 mL/kg 50% aqueous ethanol and simultaneously received the test compound by the subcutaneous route (10 mL/kg in 0.25% aqueous methyl cellulose). Thirty minutes later, they were tested for the loss of traction response (muscle relaxation) and loss of righting reflex (anesthesia). The former test consists of determining if the mouse after suspension by the forepaws on an 18 g wire can place one of its hindlimbs on the wire within 10 s. The latter test determines whether the same animal will roll over onto its feet within 10 s of release on its back. Six mice were tested at each dose, and active compounds were retested at several doses to establish an ED_{50}.

Acute Physical Dependence.[28] Male CF-1 mice (10/group) were dosed sc twice daily with the test compound, once at 0800 and again at 1600 (with 2 times the 0800 dose) for 3 days. Twenty-four hours after the last dose, they received an intravenous injection of the benzodiazepine antagonist flumazenil (2.5 mg/kg in 5% aqueous *N,N*-dimethylacetamide). Five minutes later, the electroshock seizure threshold was estimated by the up−down method in which the stimulus current was lowered or elevated by 0.05 log interval if the preceding animal did or did not convulse, respectively. From the data thus generated, a threshold (effective current of 50) was calculated. The other parameters of the transpinnal (e.g., delivered across the ears via saline-soaked ear clip electrodes) square wave stimulation were held constant (0.6 ms pulses at 100 Hz for 0.2 s). Test compounds, the precipitated withdrawal from which significantly lowered (below 95% confidence interval of parallel control group treated for 3 days with saline and injected intravenously with flumazenil) the seizure threshold, were considered to have caused physical dependence.

Benzodiazepine Antagonism. Male CF-1 Charles River mice were injected ip simultaneously with 1 mg/kg triazolam and test compound starting at 100 mg/kg. A dose−response was run on a 0.5 log scale. All drugs were made up in no. 122 sterile vehicle (0.25% aqueous methyl cellulose). Fifteen minutes later, they were tested for loss of traction response (muscle relaxation) as indicated above. If the expected loss of traction in response to triazolam was not observed, the test compound was assumed to be an antagonist. Lower doses (at 0.5 log intervals) of the test compound were then evaluated to establish the antagonist $dose_{50}$ (ED_{50}).

References

(1) (a) Squires, R., Ed. *GABA and Benzodiazepine Receptors*; CRC Press: Boca Raton, FL, 1988; Vol. I, II. (b) Haefely, W. In *Benzodiazepines*; Beaumont, G., Brandon, S., Leonard, B. E., Eds.; John Wiley and Sons: New York, 1990; pp 1−18. (c) Haefely, W. Partial Agonists of the Benzodiazepine Receptor: From Animal Data to Results in Patients. In *Chloride Channels and Their Modulation by Neurotransmitters and Drugs*; Biggio, G., Costa, E., Eds.; Raven Press: New York, 1988; pp 275−292.

(2) (a) Gardner, C. R. Functional *In Vivo* Correlates of the Benzodiazepine Agonist-Inverse Agonist Continuum. *Prog. Neurobiol.* **1988**, *31*, 425−476. (b) Braestrup, C.; Nielsen, M. In *Receptor Biochemistry and Methodology*; Olsen, R. W., Venter, J. C., Eds.; A. R. Liss, Inc.: New York, 1986; Vol. 5, p 167. (c) Bare, T. M.; Resch, J. F.; Patel, J. B. Anxiolytics and Sedative-Hypnotics. In *Annual Reports in Medicinal Chemistry;* Bailey, D. M., Ed.; Academic Press: New York, 1987; Vol. 22, pp 11−20. (d) Haefely, W.; Kyburz, E.; Gerecke, M.; Mohler, H. Recent Advances in the Molecular Pharmacology of Benzodiazepine Receptors and in the Structure-Activity Relationships of Their Agonists and Antagonists. In *Advances in Drug Research*; Testa, B., Ed.; Academic Press: New York, 1985; Vol. 14, pp 165−322. (e) Braestrup, C.; Honore, T.; Nielsen, M.; Petersen, E. N.; Jensen, L. H. Ligands for Benzodiazepine Receptors With Positive and Negative Efficacy. *Biochem. Pharmacol.* **1984**, *33*, 859−862.

(3) (a) Petersen, E. N.; Jensen, L. H.; Diejer, J.; Honore, T. New Perspectives in Benzodiazepine Receptor Pharmacology. *Pharmacopsychiatry* **1986**, *19*, 4−6. (b) Haefely, W. Psychopharmacology of Anxiety. *Eur. Neuropsychopharmacol.* **1991**, *1*, 89−95.

(4) (a) Pritchett, D. B.; Sontheimer, H.; Shivers, B. D.; Ymer, S.; Kettenmann, H.; Schonfield, P. R.; Seeburg, P. H. Importance of a Novel $GABA_A$ Receptor Subunit for Benzodiazepine Pharmacology. *Nature* **1989**, *338*, 582−585. (b) Pritchett, D. B.; Seeburg, P. H. γ-Aminobutyric Acid Type A Receptor Point Mutation Increases the Affinity of Compounds for the Benzodiazepine Site. *Proc. Natl. Acad. Sci. U.S.A.* **1991**, *88*, 1421−1425.

(5) (a) Skolnick, P.; Wong, G. In *Imidazopyridines in Anxiety Disorders: A Novel Experimental and Therapeutic Approach*; Zivkovic, B., Langer, S., Bartholini, G., Eds.; Raven Press: New York, 1992. (b) For a recent review, see: Yeh, H. H.; Grigorenko, E. V. Deciphering the Native $GABA_A$ Receptor: Is There Hope? *J. Neurosci. Res.* **1995**, *41*, 567−571.

(6) (a) TenBrink, R. E.; Im, W. B.; Sethy, V. H.; Tang, A. H.; Carter, D. B. Antagonist, Partial Agonist, and Full Agonist Imidazo[1,5-*a*]quinoxaline Amides and Carbamates Acting through the $GABA_A$/Benzodiazepine Receptor. *J. Med. Chem.* **1994**, *37*, 758−768. (b) Jacobsen, E. J.; TenBrink, R. E.; Stelzer, L. S.; Belonga, K. L.; Carter, D. B.; Im, H. K.; Im, W. B.; Sethy, V. H.; Tang, A. H.; VonVoigtlander, P. F.; Petke, J. D. High Affinity Partial Agonist Imidazo[1,5-*a*]quinoxaline Amides, Carbamates and Ureas at the $GABA_A$/Benzodiazepine Receptor Complex. *J. Med. Chem.* **1996**, *39*, 158−175.

(7) (a) Tang, A. H.; Franklin, S. R.; Himes, C. S.; Ho, P. M. Behavioral Effects of U-78875, a Quinoxalinone Anxiolytic with Potent Benzodiazepine Antagonist Activity. *J. Pharmacol. Exp. Ther.* **1991**, *259*, 248−254. (b) Petke, J. D.; Im, H. K.; Im, W. B.; Blakeman, D. P.; Pregenzer, J. F.; Jacobsen, E. J.; Hamilton, B. J.; Carter, D. B. Characterization of Functional Interactions of Imidazoquinoxaline Derivatives with Benzodiazepine-γ-Aminobutyric $Acid_A$ Receptors. *Mol. Pharmacol.* **1992**, *42*, 294−301.

(8) Ulrich, R. G.; Cramer, C. T.; Bacon, J. A.; Funk, G. M.; Hunt, C. E.; Kholmukhamedov, E.; Petrella, D. K.; Sun, E. L. Interference with Hepatocelluar Metabolism by a Quinoxalinone Anxiolytic and Its Carboxylic Acid Metabolite: What Factors Contribute Towards Cell Death? 1994 Annual Society of Toxicology Meeting, Dallas, TX, Mar. 14−17, 1994.

(9) Ulrich, R. G. Personal communication.

(10) Kyburz, E. Serendipity in Drug Discovery. The Case of BzR Ligands. *Farmaco* **1989**, *44*, 345−382.

(11) Watjen, F.; Baker, R.; Engelstoff, M.; Herbert, R.; MacLeod, A.; Knight, A.; Merchant, K.; Moseley, J.; Saunders, J.; Swain, C. J.; Wong, E.; Springer, J. P. Novel Benzodiazepine Receptor Partial Agonists: Oxadiazolylimidazobenzodiazepines. *J. Med. Chem.* **1989**, *32*, 2282−2291.

(12) Weber, W. P.; Gokel, G. W. An Improved Procedure for the Hofmann Carbylamine Synthesis of Isonitriles. *Tetrahedron Lett.* **1972**, *17*, 1637−1640.

(13) Watjen, F.; Engelstoft, M. U.S. Pat. 4,774,245, 1988. Watjen, F.; Engelstoft, M. U.S. Pat. 4,795,749, 1989.

(14) Borch, R. F.; Bernstein, M. D.; Durst, H. D. The Cyanoborohydride Anion as a Selective Reducing Agent. *J. Am. Chem. Soc.* **1971**, *93*, 2897−2904.

(15) Sethy, V. H.; Harris, D. W. Determination of Biological Activity of Alprazolam, Triazolam and Their Metabolites. *J. Pharm. Pharmacol.* **1982**, *34*, 115−116.
(16) Im, W. B.; Blakeman, D. P. Correlation Between γ-Aminobutyric $Acid_A$ Receptor Ligand-Induced Changes in t-Butylbicyclophosphoro[^{35}S]thionate Binding and $^{36}Cl^-$ Uptake in Rat Cerebrocortical Membranes. *Mol. Pharmacol.* **1991**, *39*, 394−398.
(17) Schwartz, R. D.; Suzdak, P. D.; Paul, S. M. γ-Aminobutyric Acid (GABA)- and Barbiturate-Mediated $^{36}Cl^-$ Uptake in Rat Brain Synaptoneurosomes: Evidence for Rapid Desensitization of the GABA Receptor-Coupled Chloride Ion Channel. *Mol. Pharmacol.* **1986**, *30*, 419−426.
(18) Im, H. K.; Im, W. B.; Hamilton, B. J.; Carter, D. B.; VonVoigtlander, P. F. Potentiation of GABA-Induced Chloride Currents by Various Benzodiazepine Site Agonists with $\alpha_1\gamma_2$, $\beta_2\gamma_2$ and $\alpha_1\beta_2\gamma_2$ Subtypes of Cloned $GABA_A$ Receptors. *Mol. Pharmacol.* **1993**, *44*, 866−870.
(19) Rudzik, A. D.; Hester, J. B.; Tang, A. H.; Straw, R. N.; Friis, W. Triazolobenzodiazepines, A New Class of Central Nervous System-Depressant Compounds. In *The Benzodiazepines;* Garatini, S., Mussini, E., Randall, L. O., Eds.; Raven Press: New York, 1973; pp 285−297.
(20) These standards had ED_{50}'s in the range of 0.17−4.5 mg/kg.
(21) (a) Pritchett, D. B.; Seeburg, P. H. γ-Aminobutyric $Acid_A$ Receptor α_5-Subunit Creates Novel Type II Benzodiazepine Receptor Pharmacology. *J. Neurochem.* **1990**, *54*, 1802−1804. (b) Pritchett, D. B.; Luddens, H.; Seeburg, P. H. Type I and Type II $GABA_A$-Benzodiazepine Receptors Produced in Transfected Cells. *Science* **1989**, *245*, 1389−1392.
(22) Luddens, H.; Pritchett, D. B.; Kohler, M.; Killisch, I.; Keinanen, K.; Monyer, H.; Sprengel, R.; Seeburg, P. H. Cerebellar $GABA_A$ Receptor Selective for a Behavioral Alcohol Antagonist. *Nature* **1990**, *346*, 648−651.
(23) Puia, G.; Vicini, S.; Seeburg, P. H.; Costa, E. Influence of Recombinant γ-Aminobutyric $Acid_A$ Receptor Subunit Composition on the Action of Allosteric Modulators of γ-Aminobutyric $Acid_A$-Gated Cl^- Currents. *Mol. Pharmacol.* **1991**, *39*, 691−696.
(24) Carter, D. B.; Thomsen, D. R.; Im, W. B.; Lennon, D. J.; Ngo, D. M.; Gale, W.; Im, H. K.; Seeburg, P. H.; Smith, M. W. Functional Expression of $GABA_A$ $Chloride^-$ Channels and Benzodiazepine Binding Sites in Baculovirus Infected Insect Cells. *Bio/Technology* **1992**, *10*, 679−681.
(25) Hamilton, B. J.; Lennon, D. J.; Im, H. K.; Im, W. B.; Seeburg, P. H.; Carter, D. B. Stable Expression of Cloned Rat $GABA_A$ Receptor Subunits in a Human Kidney Cell Line. *Neurosci. Lett.* **1993**, *153*, 206−209.
(26) Jacobsen, E. J.; TenBrink, R. E.; Stelzer, L. S.; Belonga, K. B.; Carter, D. B.; Im, H. K.; Im, W. B.; Sethy, V. H.; Tang, A. H.; VonVoigtlander, P. F.; Petke, J. D. Unpublished observations.
(27) Im, H. K.; Im, W. B.; Pregenzer, J. F.; Carter, D. B.; Jacobsen, E. J.; Hamilton, B. J. Characterization of U-97775 as a $GABA_A$ Receptor Ligand of Dual Functionality in Cloned Rat $GABA_A$ Receptor Subtypes. *Br. J. Pharmacol.* **1995**, *115*, 19−24.
(28) (a) VonVoigtlander, P. F.; Lewis, R. A. A Rapid Screening Method for the Assessment of Benzodiazepine Receptor-Related Physical Dependence in Mice. *J. Pharmacol. Methods.* **1991**, *26*, 1−5. (b) Fialip, J.; Aumaitre, O.; Eschalier, A.; Maradeix, B.; Dordain, G.; Lavarenne, J. Benzodiazepine Withdrawal Seizures: Analysis of 48 Case Reports. *Clin. Neuropharmacol.* **1987**, *10*, 538−544.
(29) Mohamadi, F.; Richards, N. G. J.; Guida, W. C.; Liskamp, R.; Lipton, M.; Caufield, C.; Chang, G.; Hendrickson, T.; Still, W. C. MacroModel-An Integrated Software System for Modeling Organic and Bioorganic Molecules Using Molecular Mechanics. *J. Comput. Chem.* **1990**, *11*, 440−467.
(30) Weiner, S. J.; Kollman, P. A.; Nguyen, D. T.; Case, D. A. An All Atom Force Field for Simulations of Proteins and Nucleic Acids. *J. Comput. Chem.* **1986**, *7*, 230−252.
(31) Allinger, N. L. Conformational Analysis. 130. MM2: A Hydrocarbon Force Field Utilizing V_1 and V_2 Torsional Terms. *J. Am. Chem. Soc.* **1977**, *99*, 8127−8134.
(32) Chang, G.; Guida, W. C.; Still, W. C. An Internal Coordinate Monte Carlo Method for Searching Conformational Space. *J. Am. Chem. Soc.* **1989**, *111*, 4379−4386.
(33) Tebib, S.; Bourguignon, J.-J.; Wermuth, C.-G. The Active Analog Approach Applied to the Pharmacophore Identification of Benzodiazepine Receptor Ligands. *J. Comput.-Aided Mol. Des.* **1987**, *1*, 153−170.
(34) Gardner, C. R. A Review of Recently-Developed Ligands for Neuronal Benzodiazepine Receptors and Their Pharmacological Activities. *Prog. Neuro.-Psychopharmacol. Biol. Psychiatry* **1992**, *16*, 755−781.
(35) Villar, H. O.; Uyeno, E. T.; Toll, L.; Polgar, W.; Davies, M. F.; Loew, G. H. Molecular Determinants of Benzodiazepine Receptor Affinities and Anticonvulsant Activities. *Mol. Pharmacol.* **1989**, *36*, 589−600.
(36) Zhang, W.; Koehler, K. F.; Harris, B.; Skolnick, P.; Cook, J. M. Synthesis of Benzo-Fused Benzodiazepines Employed as Probes of the Agonist Pharmacophore of Benzodiazepine Receptors. *J. Med. Chem.* **1994**, *37*, 745−757.
(37) Brown, H. C.; Yoon, N. M. Selective Reductions. X. Reaction of Aluminum Hydride with Selected Organic Compounds Containing Representative Functional Groups. Comparison of the Reducing Characteristics of Lithium Aluminum Hydride and Its Derivatives. *J. Am. Chem. Soc.* **1966**, *88*, 1464−1472.
(38) Determined by ^{1}H NMR integration of the imidazole methine protons at δ 8.43 and 9.13 for the product and starting material, respectively.
(39) Pure **19c** was prepared by resubmitting a portion of the crude product mixture to the reaction conditions.

JM960070+